Project Notes:

Project Title: AI-Controlled Deployable Vortex Generators for Adaptive Airflow Optimization on Airfoils

Name: Kasam, Ishan

Knowledge Gaps:

This list provides a brief overview of the major knowledge gaps for this project, how they were resolved, and where to find the information.

Knowledge Gap	Resolved By	Information is located	Date resolved
Knowledge on Boundary layer conditions	Reading research articles	In the project notes, articles about machine learning for predicting fluid flow	10/8/2025
Knowledge on testing strategies for predicting flow over airfoils	Reading research articles	In the project notes, articles about machine learning for predicting fluid flow	10/8/2025
Knowledge on vortex generators and deployable vortex generators	Reading research articles	In the project notes, in the article about deployable vortex generators	10/1/2025

Literature Search Parameters:

These searches were performed between 06/20/2025 and XX/XX/2026.
List of keywords and databases used during this project.

Database/search engine	Keywords	Summary of search
Gordon Library	Deep learning AND Flow	Found articles which I will review in my project, I found articles that outline a method similar to what I will employ.
Gordon Library	Deployable AND Vortex Generators	I found my article about deployable vortex generators using TSAMs which were directional in deciding what I want to solve in my project
Google	Boundary layer	I learned the basics on boundary layer conditions and how they work as well as how vortex generators influence the boundary layer

Article #1 Notes: FEM-Aided Modeling and Control of a Tethered Hydrokinetic Energy Kite

Source Title	FEM-Aided Modeling and Control of a Tethered Hydrokinetic Energy Kite by David Olinger
Source citation (APA Format)	Torres, G. A., Olinger, D. J., & Demetriou, M. A. (2023). FEM-Aided modeling and control of a tethered hydrokinetic energy KITE. *2022 American Control Conference (ACC)*, 3703–3708. https://doi.org/10.23919/acc55779.2023.10156594
Original URL	https://ieeexplore.ieee.org/abstract/document/10156594
Source type	Journal Article
Keywords	Hydrokinetic energy, wave energy converter, renewable energy, modeling
#Tags	#wave_energy_conversion #hydrodynamics #fem #modeling
Summary of key points + notes (include methodology)	This research develops a model of a tethered hydrokinetic energy kite, focusing on the dynamics of both the kite and its tether to optimize energy conversion from ocean currents. The kite is treated as a rigid body, with its position described using spherical coordinates and its orientation tracked via Euler angles, while hydrodynamic forces, buoyancy, tether tension, and added mass are incorporated into the motion equations. Finite-element analysis is applied to the tether as an Euler-Bernoulli beam, converting PDEs (partial differential equations) to ODEs (ordinary differential equations) and capturing bending, tension, and distributed load effects. Lift and drag forces are calculated using finite-wing theory with induced drag, apparent flow is used to account for relative fluid velocity, and two-way coupling ensures accurate kite-tether interaction. The study found that tether dynamics significantly influence kite motion, added mass is critical for realistic acceleration predictions, and lift, drag, and tether forces together determine optimal trajectories and energy extraction efficiency.
Research Question/Problem/ Need	Previous models of kites regarded the tether and the kite as one lumped body, even though that limits the accuracy of predictions of kite behavior. This research hopes to create a detailed model of a kite that incorporates

	stretching of the tether to predict the motion of the kite while taking into account buoyancy, hydrodynamics, added mass, and the kite-tether coupling.
Important Figures	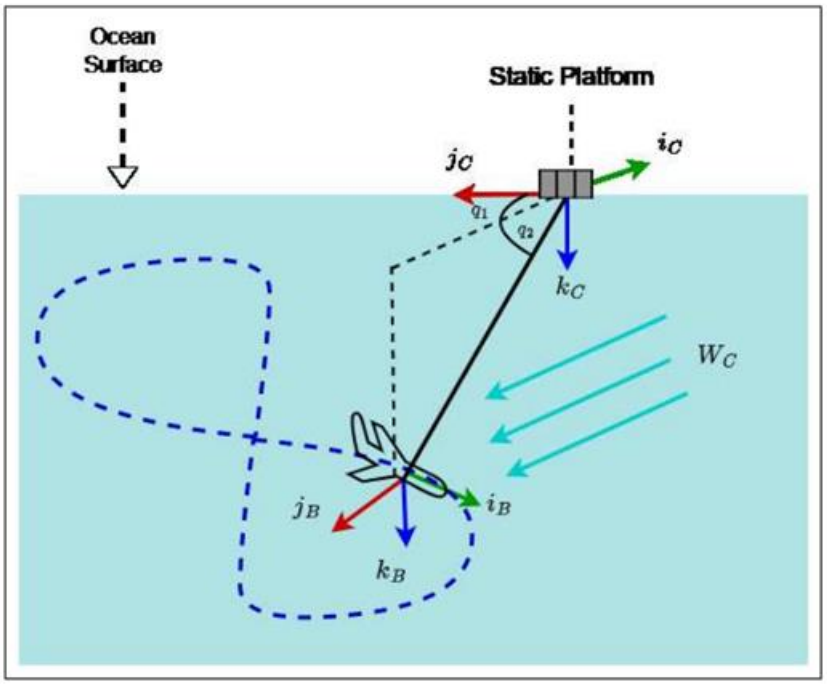 Fig. 1. TUSK Coordinate and Baseline Problem Description 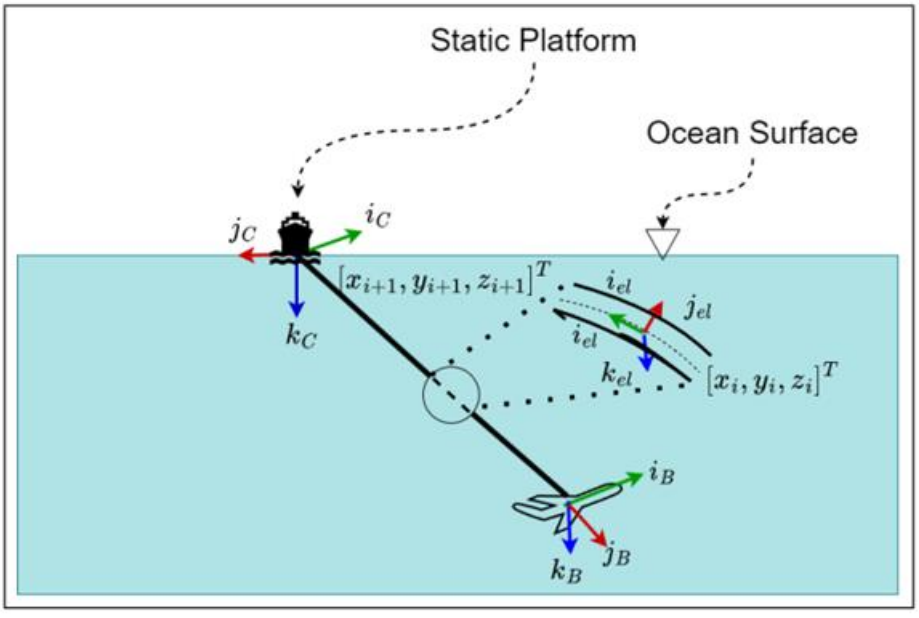 Fig. 2. Reference frames for the tether-kite modeling.

VOCAB: (w/definition)	• Tethered kite: A kite attached to a fixed point via a tether • Degrees of Freedom (DOF): Independent ways in which an object can move. For example, a set of three angles (roll, pitch, yaw) has 3 degrees of freedom. In this paper, the kite has 6 degrees of freedom • Euler angles: (roll, pitch, yaw) angles, which are used to describe an object's orientation in space • Finite-Element Method (FEM): A numerical technique in simulations that divides a structure into discrete elements to solve equations on the smaller elements to describe stress, deformation, and motion • Euler-Bernoulli Beam: A structural model used to describe the bending and tension of beams or tethers under loads • Apparent flow: The relative velocity of the fluid as seen by the moving body, which is used to calculate the lift and drag • Two-Way Coupling: A mechanism where two connected systems influence each other's motion through actions and reactions • Finite Wing Theory: An aerodynamic theory applied to wings or lifting surfaces that accounts for lift, drag, and induced drag due to finite span • Partial differential equations (PDEs): Equations that are very difficult to solve and involve rates of change with multiple variables, often used to describe motion, bending, stretching, or any dynamic behavior
Cited references to follow up on	Olinger, D. J., & Wang, Y. (2015). Hydrokinetic energy harvesting using tethered undersea kites. Journal of Renewable and Sustainable Energy, 7(4), 043114. https://doi.org/10.1063/1.4922324 Vermillion, C., Cobb, M., Fagiano, L., & Demetriou, M. A. (2021). Electricity in the air: Insights from two decades of advanced control research and experimental flight testing of airborne wind energy systems. Annual Review of Control, Robotics, and Autonomous Systems, 4, 1–30. https://doi.org/10.1146/annurev-control-061520-045348
Follow-up Questions	1. How sensitive are the kite's dynamics and energy output predictions to variations in tether stiffness, length, or added mass parameters, and could these parameters be manipulated for different ocean conditions? 2. What practical drawbacks are there when trying to convert simulation data into real-life products? 3. How does the two-way tether coupling influence control strategies, and what alternative control methods can be applied to improve the kite's performance?

Article #2 Notes: HPA-MPC: Hybrid Perception-Aware Nonlinear Model Predictive Control for Quadrotors with Suspended Loads

Source Title	HPA-MPC: Hybrid Perception-Aware Nonlinear Model Predictive Control for Quadrotors with Suspended Loads
Source citation (APA Format)	Sarvaiya, M., Li, G., & Loianno, G. (2024). HPA-MPC: Hybrid Perception-Aware Nonlinear Model Predictive Control for Quadrotors with Suspended Loads. *IEEE Robotics and Automation Letters*, 1–8. https://doi.org/10.1109/lra.2024.3505816
Original URL	https://ieeexplore.ieee.org/document/10766615?denied=
Source type	Journal article
Keywords	Model Predictive Control, UAV, Suspended Load
#Tags	#MPC_Predictions, #Dynamic_Modeling, #ML, #hybrid_dynamics #predictive_control #aerodynamics #UAV
Summary of key points + notes (include methodology)	This research is about developing a hybrid, perception-aware nonlinear model predictive control (HPA-MPC) framework for quadrotor UAVs carrying cable-suspended loads, addressing the shortcomings of prior methods that assumed always-taut cables or required external motion capture. The system models both taut and slack cable dynamics separately (hybrid) pendulum-like constrained motion in the taut case and decoupled payload/free-fall motion in the slack case, with mode switching handled by a hybrid detector, which is useful to ensure accuracy. Model predictive control (MPC) is used because it handles nonlinearities, constraints, and multiple objectives, with a cost function balancing payload tracking, quadrotor stability, and perception-awareness to keep the payload in the camera's field of view. State estimation is achieved using visual-inertial odometry and Kalman filters, while the control pipeline integrates sensing, hybrid mode detection, MPC optimization, and motor actuation in real time at 150 Hz. The experiments demonstrated smooth slack-taut transitions, sub-7 cm trajectory tracking accuracy, onboard-only deployability, and robustness against disturbances where traditional controllers fail.

Research Question/Problem/ Need	The problem is that most prior controllers either assume the cable is always taut (pendulum-like dynamics) or require external tracking systems. These assumptions fail in real-world scenarios where cables can go slack and where the vehicle must rely only on onboard sensors.
Important Figures	 Fig. 1. Robot dual hybrid states (left). The robot on the right is in the taut state while the robot on the left is in the slack state. Snapshots showing a human-interaction task where the quadrotor tracks the load as a user manipulates it via a gripper (center). An experiment where we apply a vertical disturbance to a payload as the robot executes a trajectory (right). 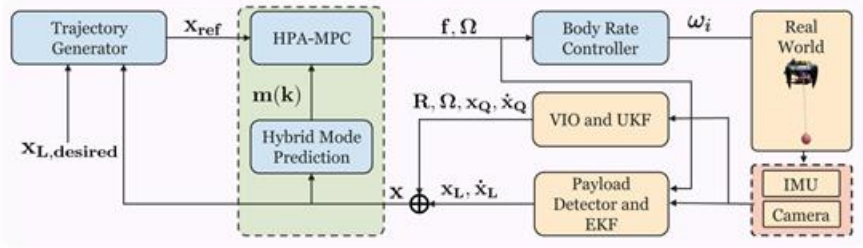 Fig. 3. The system architecture describing the flow of information through the various components of our pipeline.
VOCAB: (w/definition)	• Kalman Filter: An algorithm that estimates the state of a filter by combining predictions from a model with noisy measurements • Model Predictive Control (MPC): A control method that optimizes the behavior of a system in the future by solving a constrained optimization problem at each time stamp • Hybrid dynamics: Behavior in systems that combine continuous nonlinear motion with discrete switching events, here due to transitions between taut and slack cable modes • Perception-aware cost: A term added to the MPC optimization objective that encourages the control policy to keep the payload within the onboard camera's field of view, ensuring robust visual tracking during flight • Full state estimation: The process of determining all the necessary variables to determine a state • Prediction horizon: The future time window over which MPC predicts system behavior • Control horizon: The number of future moves optimized by MPC at each step

Cited references to follow up on	Fagiano, L., & Marks, R. (2015). *A comprehensive dynamic model of tethered wings for airborne wind energy*. IEEE Transactions on Control Systems Technology, 23(4), 1433–1447. https://doi.org/10.1109/TCST.2014.2362251 Vermillion, C., Cobb, M., Fagiano, L., & Demetriou, M. A. (2021). *Electricity in the air: Insights from two decades of advanced control research and experimental flight testing of airborne wind energy systems*. Annual Review of Control, Robotics, and Autonomous Systems, 4, 1–30. https://doi.org/10.1146/annurev-control-062820-084246
Follow-up Questions	1. How would other filtering methods aside from Kalman filters perform for processing noisy data? 2. How can CFD play a role in training a model to respond to wind conditions? 3. Could additional perception constraints, such as multiple camera angles or depth sensing, further enhance payload tracking during aggressive maneuvers or external disturbances?

Article #3 Notes: Effect of unsteady pressure rise on flame propagation and near-cold-wall ignition

Source Title	**Effect of unsteady pressure rise on flame propagation and near-cold-wall ignition**
Source citation (APA Format)	Jayachandran, J., & Egolfopoulos, F. N. (2018). Effect of unsteady pressure rise on flame propagation and near-cold-wall ignition. *Proceedings of the Combustion Institute*, *37*(2), 1639–1646. https://doi.org/10.1016/j.proci.2018.06.065
Original URL	https://www.sciencedirect.com/science/article/pii/S1540748918302487
Source type	Journal Article
Keywords	Near-cold-wall ignition, combustion, pressure rise, flame propagation
#Tags	#unsteady_pressure_rise, #negative_temperature_coefficient, #numerical_study
Summary of key points + notes (include methodology)	This research is about how unsteady pressure rises in combustion engines affect flame propagation speed and near-cold wall ignition, addressing the limitations of previous studies that assumed quasi-steady flame behavior. The study uses one-dimensional conservation equations for mass, species, and energy with imposed dP/dt boundary conditions, allowing for the pressure rise effects to be isolated. The study uses hydrogen for fast flame propagation and n-heptane to show NTC behavior. All of the work done in this study was computational, and the methods include using PREMIX for steady flames, SENKIN for ignition delays, and DASPK for time integration, with chemical kinetics from previous work. The results show that rapid pressure rise enhances mass burning flux nearly linearly with pressure rise number, and that rapid pressure rise alters ignition location between the main gas and the thermal boundary layer, and produces hotter reaction zones due to non-uniform compression. The study demonstrates that quasi-steady assumptions fail, highlighting the need for corrections in flame propagation and knock prediction models, with regime diagrams and PRN frameworks.
Research Question/Problem/ Need	The problem is filling the knowledge gap where previous studies assumed quasi-steady flame behavior, ignoring the dynamic effects of rapid pressure changes of real flames. These assumptions would fail in

	modern engines where the pressure rise rate is high, and this study isolates the effects of pressure rise rate.
Important Figures	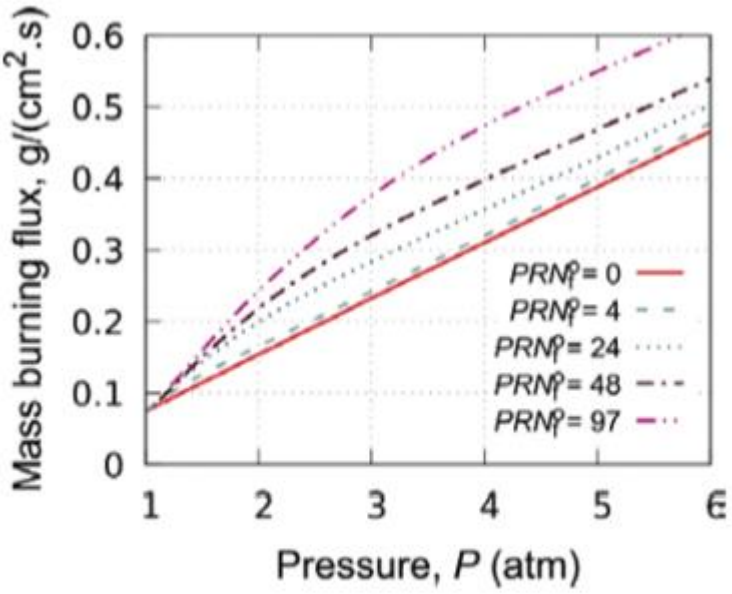 Fig. 1. $\dot{m}$ as a function of P for the $\phi = 0.6$, H_2/air mixture with $T_u^o = 300$ K, $P^o = 1$ atm for different values of PRN_f^o. 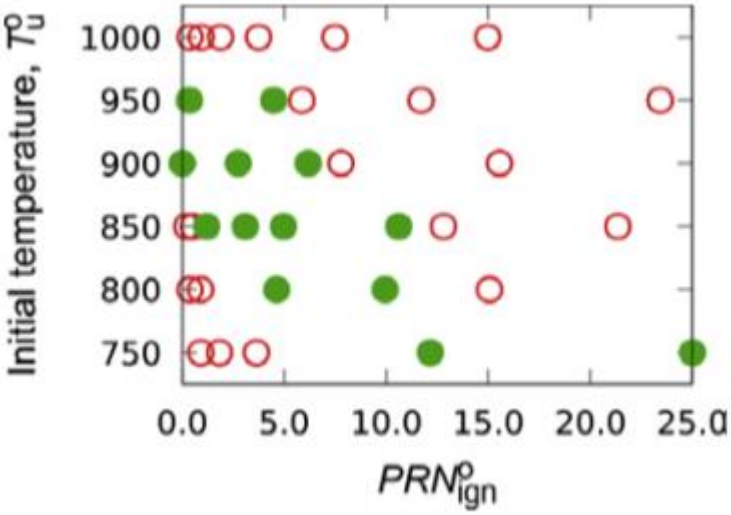
VOCAB: (w/definition)	• Unsteady pressure rise: A rapid change in pressure over time rather than a constant or slowly changing pressure

	• Flame propagation: The speed and manner in which a flame moves through a fuel-air mixture • Near-cold-wall-ignition: The process of a fuel-air mixture igniting close to the cooler walls of a combustion chamber • dP/dt: Change in pressure • NTC (Negative Temperature Coefficient): A chemical reaction phenomenon where lowering the temperature can temporarily increase the reaction rate • Mass burning flux: The amount of fuel burned per unit of area per unit of time • Thermal boundary layer: The thin layer of cool gas near the wall of a combustion chamber • PRN (Pressure rise number): A dimensionless parameter representing the rate of pressure rise in the system • Knock: A damaging engine condition caused by uncontrolled ignition
Cited references to follow up on	None
Follow-up Questions	1. How can cold-wall ignition mechanisms evolve to be used in simulations with more realistic engine conditions, such as walls with varying temperature gradients? 2. How would the results change if different fuels were used? 3. How transferable are these findings into real-life systems, and what still needs to be explored to implement this into a real engine?

Article #4 Notes: Minimum-Time Sequential Traversal by a Team of Small Unmanned Aerial Vehicles in an Unknown Environment with Winds

Source Title	Minimum-Time Sequential Traversal by a Team of Small Unmanned Aerial Vehicles in an Unknown Environment with Winds
Source citation (APA Format)	DesRoches, J. A., & Cowlagi, R. V. (2025). Minimum-Time Sequential Traversal by a Team of Small Unmanned Aerial Vehicles in an Unknown Environment with Winds. *arXiv (Cornell University)*. https://doi.org/10.48550/arxiv.2501.09944
Original URL	https://arxiv.org/abs/2501.09944
Source type	Journal article
Keywords	Autonomous, UAV, winds, sequential traversal
#Tags	#Autonomous_UAV, #machine_learning, #physics_trained, #minimum_time_traversal, #coordinated_robots
Summary of key points + notes (include methodology)	This research is about the development of a sequential planner for a team of UAVs to minimize traversal time from a fixed start to a fixed goal in an urban area with unknown, time-varying winds. The urban area is modeled as a 2D grid graph where edges represent street segments with traversal times influenced by wind, and the UAVs fly at fixed air relative speeds while recording wind measurements along edges. Wind is simplified using a single time-varying global driving signal with edge-specific scale factors, and static edge costs are computed from averaged measurements or polynomial-stitched segments to allow for planning. Each UAV's measurements update a central agent, which recalculates optimal paths using Dijkstra's algorithm, and the methodology includes Kalman filtering of the global driver signal as an alternative to polynomial stitching for handling periodic signals. Different simulations vary grid size, street length, UAV speed, wind speed, and measurement noise to evaluate convergence in different conditions. The study found that larger grids and more measurement noise required more UAVs to update the central agent before the model could accurately handle the conditions.
Research Question/Problem/ Need	The problem is that previous sequential UAV systems assume static wind conditions, leaving a knowledge gap regarding path planning for multiple

	UAVs in urban environments. Previous studies used sequential UAVs to update the robot prior to the model for all of them.
Important Figures	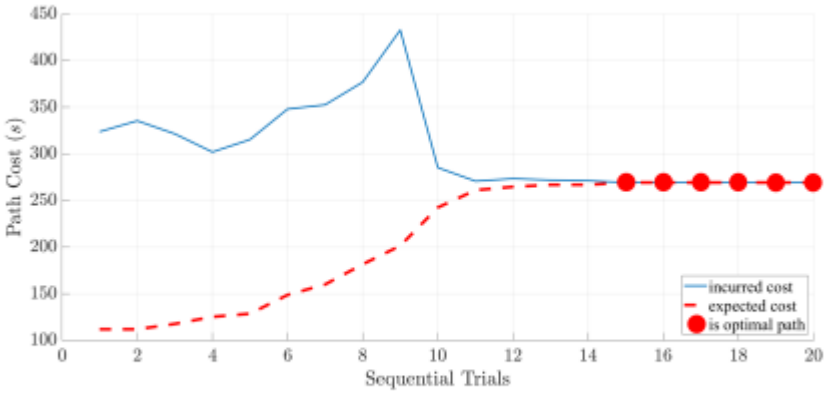 Fig. 4. Expected vs incurred path cost for environment Case 1, 9×9 grid. 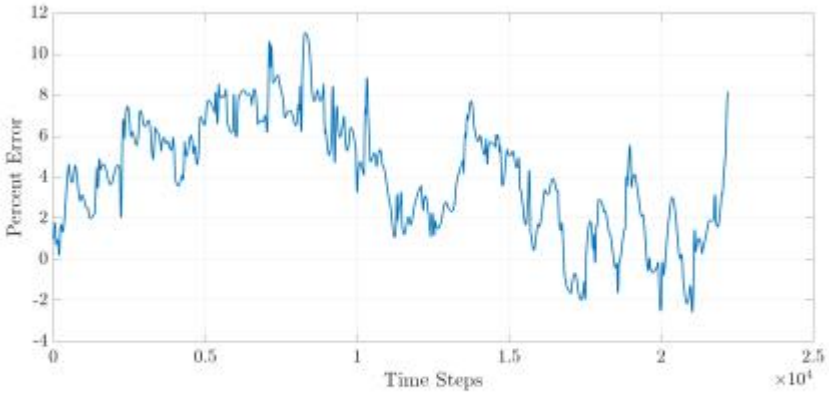 Fig. 6. Percent error between the estimated and true $P_{x_2}(t)$ for a 5×5 grid, Case 4 without a Kalman Filter.
VOCAB: (w/definition)	• Vertex: A point or a node in a graph • Edge: A line connecting two nodes in a graph • Dijkstra's algorithm: A method for finding the shortest path between points in a weighted graph • Static edge costs: Pre-calculated, fixed values for how long it takes to traverse a path in a graph • Polynomial stitching: A method of combining small data segments into one smooth estimate using curves • Kalman filter: An algorithm that estimates the current state of a changing system by combining predictions with noisy measurements

	• State representation: The set of values, like position, speed, acceleration, etc., that describes a system at a given moment • UAV: A drone that flies without a person on board • Air-relative speed: The speed of the UAV relative to the surrounding air • Pressure gradient surrogate: A simplified number used to estimate how wind changes over an area without actually measuring the wind everywhere • Anti-symmetric wind: Wind that blows equally in opposite directions along a path • Process uncertainty: An estimate of how much a system might change unpredictably between measurements • Sequential traversal: UAVs flying one after another • Central agent: A system that collects data from UAVs and calculates the best paths for future flights • Driving signal/global driver: The underlying pattern that represents how wind changes across the environment
Cited references to follow up on	M. Rakib, S. Evans, and P. Clausen, “Measured gust events in the urban environment, a comparison with the iec standard,” Renewable Energy, vol. 146, pp. 1134–1142, 2020. Korprasertsak, Natapol and Leephakpreeda, Thananchai, “Improving accuracy of wind analysis with multiple sampling rates of wind measurement,” E3S Web Conf., vol. 95, p. 02002, 2019.
Follow-up Questions	1. What new factors might have to be taken into account when implementing this system on a real team of drones? 2. How sensitive is the method to sensor errors in measuring airspeed and ground speed, and how would these difficulties be mitigated? 3. In real life, how would energy constraints affect the design and performance of the UAVs and the path planning algorithm?

Article #5 Notes: Micropulsed Plasma Thrusters for Attitude Control of a Low-Earth-Orbiting CubeSat

Source Title	Micropulsed Plasma Thrusters for Attitude Control of a Low-Earth-Orbiting CubeSat
Source citation (APA Format)	Gatsonis, N. A., Lu, Y., Blandino, J., Demetriou, M. A., & Paschalidis, N. (2016). Micropulsed plasma thrusters for attitude control of a Low-Earth-Orbiting CubeSAT. *Journal of Spacecraft and Rockets*, *53*(1), 57–73. https://doi.org/10.2514/1.a33345
Original URL	https://www.researchgate.net/publication/290244379_Micropulsed_Plasma_Thrusters_for_Attitude_Control_of_a_Low-Earth-Orbiting_CubeSat
Source type	Journal Article
Keywords	Plasma Thrusters, CubeSat, Attitude Control
#Tags	#CubeSat, #AttitudeControl, #EfficientFrameworks
Summary of key points + notes (include methodology)	This article explores how micropulsed plasma thrusters can be used to overcome the limitations of traditional magnetic torquers in CubeSat attitude control. Using Teflon propellant and Lorentz-force acceleration, micropulsed plasma thrusters achieve high exhaust velocity and specific impulse while consuming very little mass. The researchers designed a CubeSat system around an eight-thruster dual-layer configuration, supported by deployable solar panels and commercial-grade sensors, and tailored control algorithms to account for the thrusters' pulsed operation. Simulations showed rapid detumbling, sub-degree pointing accuracy, efficient energy use, and resilience to multiple thruster failures, demonstrating μPPTs as a reliable and scalable solution for CubeSat usage in low Earth orbit.
Research Question/Problem/ Need	Traditional magnetic torquers have dead zones and can not ensure robust pointing during Earth-orbiting missions. These gaps in control can make many missions fail, so micropulsed plasma thrusters were used to provide torque without the dead zones.

Important Figures

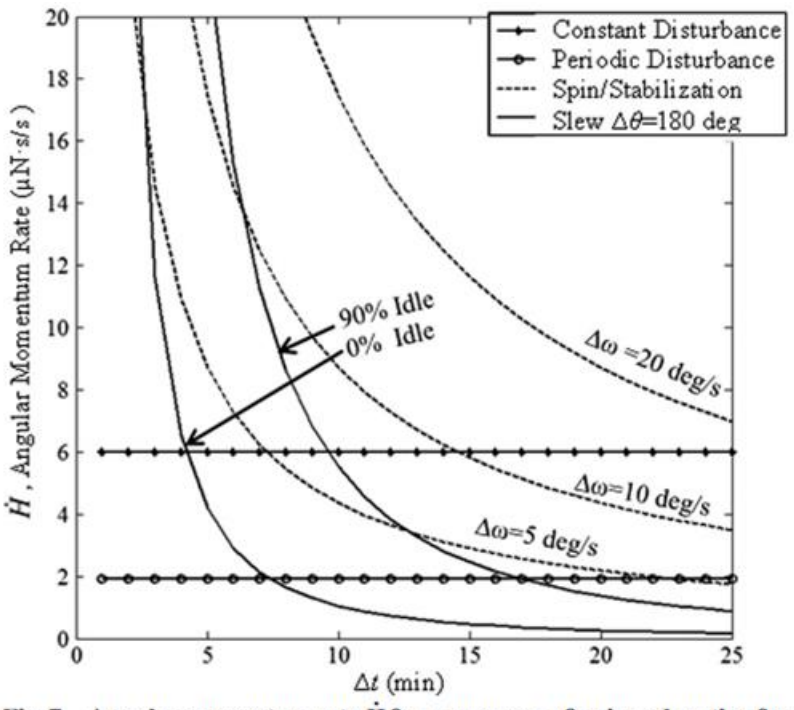

Fig. 7 Angular momentum rate $\dot{H}$ for maneuvers of a given duration for the 3U Cubesat shown in Fig. 1b.

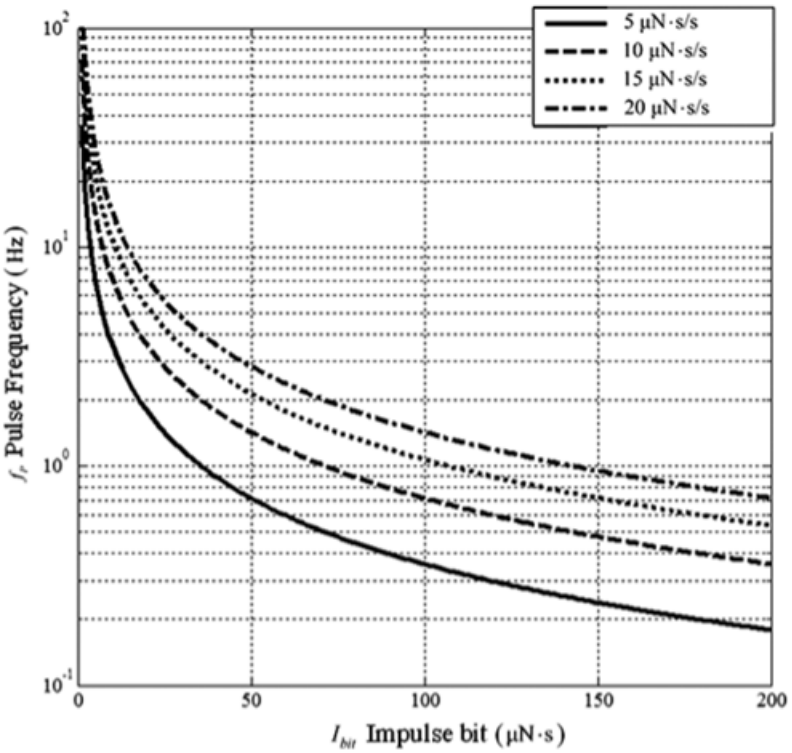

Fig. 8 Required impulse bit and pulse frequency for different angular momentum rates of a 3U CubeSat shown in Fig. 1b.

VOCAB: (w/definition)	• CubeSat: A small satellite built from standardized 10 cm cubic units, designed for low cost and mass production • Attitude control: The process of regulating a spacecraft's orientation in space by generating torques about its axes • Quaternion: A mathematical method for describing spacecraft orientation in three dimensions without singularities • Micropulsed plasma thruster: A device that removes solid Teflon with electrical discharges to create pulsed plasma jets for precise thrust • Impulse bit: The momentum change delivered by a single thruster pulse • Lorentz force: The force on charged particles caused by electric and magnetic field interactions, used to accelerate plasma in thrusters • Specific impulse: A measure of propulsion efficiency, defined as thrust per unit of propellant consumption • Moment arm: The perpendicular distance between where a force is applied and the axis of rotation, determining the torque produced • Extended Kalman Filter (EKF): An algorithm that combines noisy sensor data with system models to estimate spacecraft orientation and angular velocity
Cited references to follow up on	Shaw, P. V., and Lappas, V. J., "Design, Development and Evaluationof an 8 µPPT Propulsion Module for a 3U CubeSat Application," 31stInternational Electric Propulsion Conference, IEPC Paper 2011-115,2011.
Follow-up Questions	Why are micropulsed plasma thrusters not widely used in CubeSat propulsion? How would plasma thrusters work on larger models?

Article #6 Notes: OriSnake: Design, Fabrication, and Experimental Analysis of a 3-D Origami Snake

Source Title	OriSnake: Design, Fabrication, and Experimental Analysis of a 3-D Origami Snake
Source citation (APA Format)	Ming Luo, Ruibo Yan, Zhenyu Wan, Yun Qin, Santoso, J., Skorina, E. H., & Onal, C. D. (2018). OriSnake: Design, Fabrication, and Experimental Analysis of a 3-D Origami Snake Robot. *IEEE Robotics and Automation Letters*, *3*(3), 1993–1999. https://doi.org/10.1109/LRA.2018.2800112
Original URL	https://ieeexplore-ieee-org.ezpv7-web-p-u01.wpi.edu/document/8276287
Source type	Journal Article
Keywords	Origami
#Tags	#Soft_Robotics, #Cable_Actuation, #Snake_Robot
Summary of key points + notes (include methodology)	This study is about the creation of OriSnake, a modular, cable driven robot that uses aspects of origami. Yoshimura bellows modules were used to provide bending compliance and built in structural antagonism without the need for springs. The robot was fabricated from laser cut PET (a type of plastic) sheets, using DC motors, passive wheels for anisotropic friction, and a control system using an Arduino controller. The testing for this robot analyzed the optimal serpentine locomotion using curvature laws and gait sweeps with different parameters, with the results showing that the snake was fastest at 60 degree bending amplitude and 50 degree phase offset. The authors included that performance was hindered by motor selection and fabrication tolerances.
Research Question/Problem/ Need	Reducing the weight and complexity or traditional snake robots while exploring lightweight, low-cost, serpentine locomotion.

Important Figures	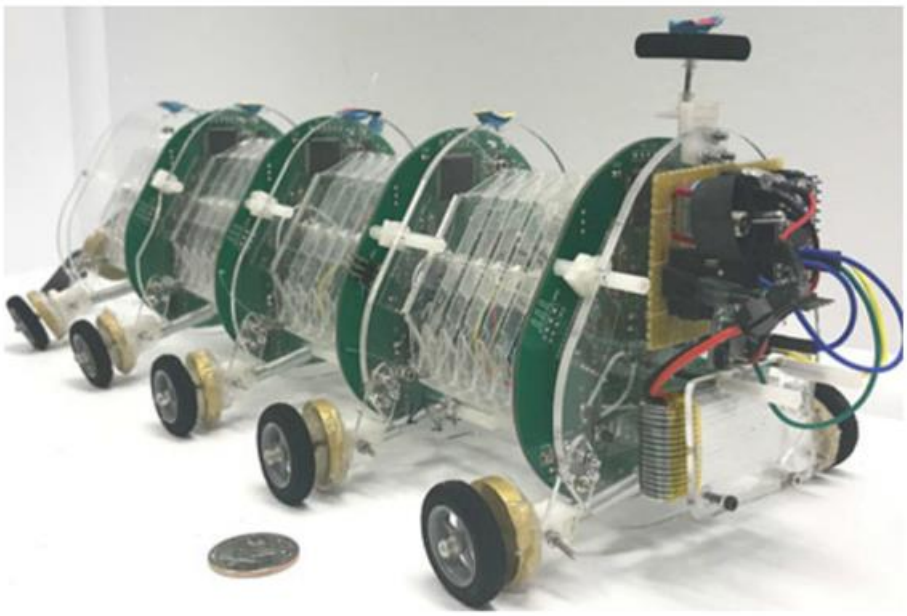 Fig. 1. The 3D origami snake robot. 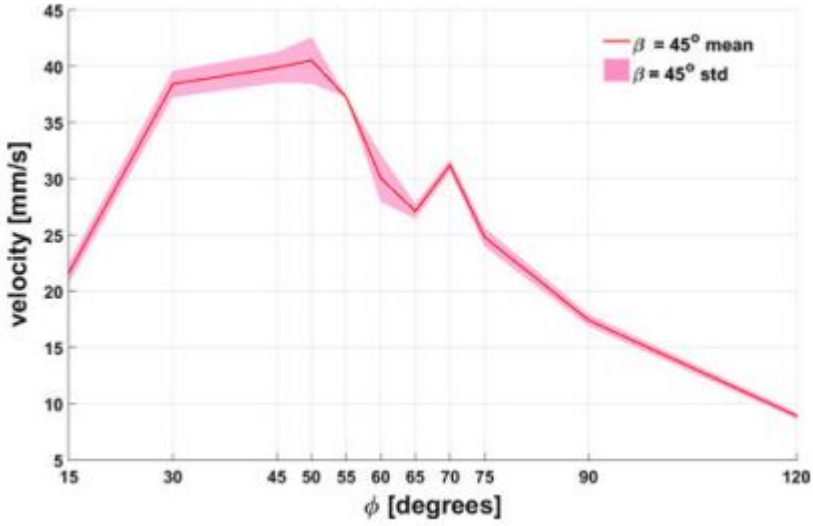
VOCAB: (w/definition)	• Yoshimura bellows modules: Origami crease patterns that are used to enable bending and axial compliance while resisting torsion • Structural antagonism: Passive mechanical resistance that restores body shape without additional force • Anisotropic friction: Unequal friction forces with higher lateral than longitudinal forces that are used for locomotion • Serpentine curvature law: The mathematical description of the movement of a snake as a sine wave

	• PID control: Proportional, Integral, Derivative control which is used to smooth out motions • Inverse kinematics: Modeling of a desired motion while assuming all geometry is rigid • Cable driven actuation: Motion generated by pulling cables arranged in a triangular layout • Backlash: Mechanical play or looseness in a gear system
Cited references to follow up on	R. Crespi and A. J. Ijspeert, "Amphibot ii: An amphibious snake robot that crawls and swims using a central pattern generator," in Proc. 9th Int. Conf. Climbing Walking Robots, no. BIOROB-CONF-2006-001, 2006, pp. 19–27. C. D. Onal, R. J. Wood, and D. Rus, "An origami-inspired approach to worm robots," IEEE/ASME Trans. Mechatronics, vol. 18, no. 2, pp. 430– 438, Apr. 2013.
Follow-up Questions	Could OriSnake be modified to include active wheels for increased traction without major drawbacks? How could this design possibly be improved to accommodate a wider range or terrains?

Article #7 Notes: A Shared Autonomous Nursing Robot Assistant with Dynamic Workspace for Versatile Mobile Manipulation

Source Title	A Shared Autonomous Nursing Robot Assistant with Dynamic Workspace for Versatile Mobile Manipulation
Source citation (APA Format)	N. Boguslavskii, Z. Zhong, L. M. Genua and Z. Li, “A Shared Autonomous Nursing Robot Assistant with Dynamic Workspace for Versatile Mobile Manipulation,” 2023 IEEE/RSJ International Conference on Intelligent Robots and Systems (IROS), Detroit, MI, USA, 2023, pp. 7040-7045, doi: 10.1109/IROS55552.2023.10342401.
Original URL	https://ieeexplore-ieee-org.ezpv7-web-p-u01.wpi.edu/document/10342401
Source type	Journal Article
Keywords	Navigation;Robot kinematics;Robot vision systems;Humanoid robots;Collision avoidance;Usability;Task analysis
#Tags	#AutonomousAssistiveRobot, #HybridOperation, #DC_Actuation
Summary of key points + notes (include methodology)	This study explores a shared autonomous nursing robot with a motorized chest and dual 7 DOF arms to extend its vertical workspace intended to assist in and manipulate things in hospital environments. The system uses ROS and Unity for control and uses onboard sensing for untethered operation, and employs shared autonomous that coordinate with human efforts. Testing in a virtual hospital testbed across eight benchmark nursing tasks showed that autonomy improved efficiency in precision-heavy tasks while navigation tasks performed similarly under direct or autonomous control. Physical trials showed that the scaling method allowed faster task completion than proximity control, though it increased operator fatigue, showing a tradeoff between efficiency and usability.
Research Question/Problem/ Need	Nurses in hospitals face routine and physically and cognitively demanding work, and current robots lack reach and versatility.

Important Figures	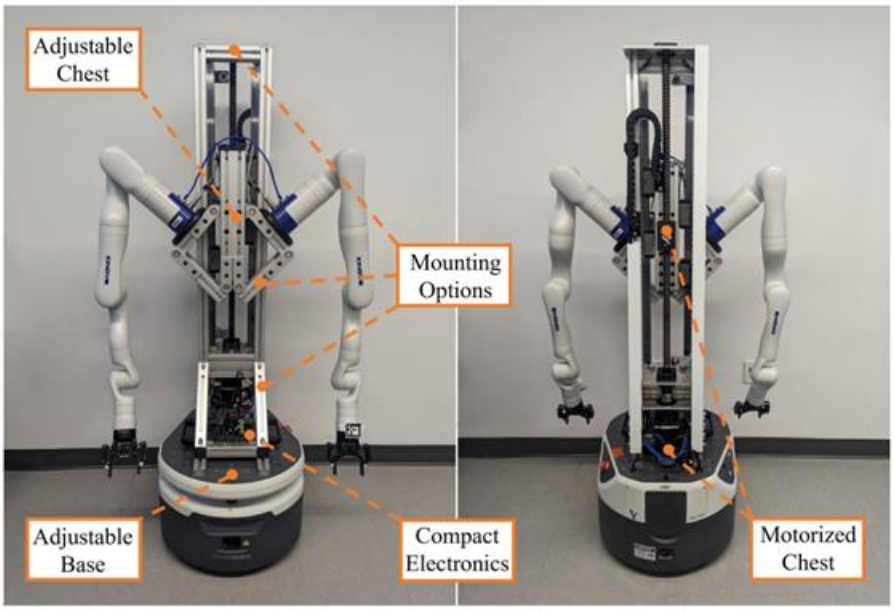 Fig. 1: Nursing assistance robot with versatile supporting structure and motorized chest. 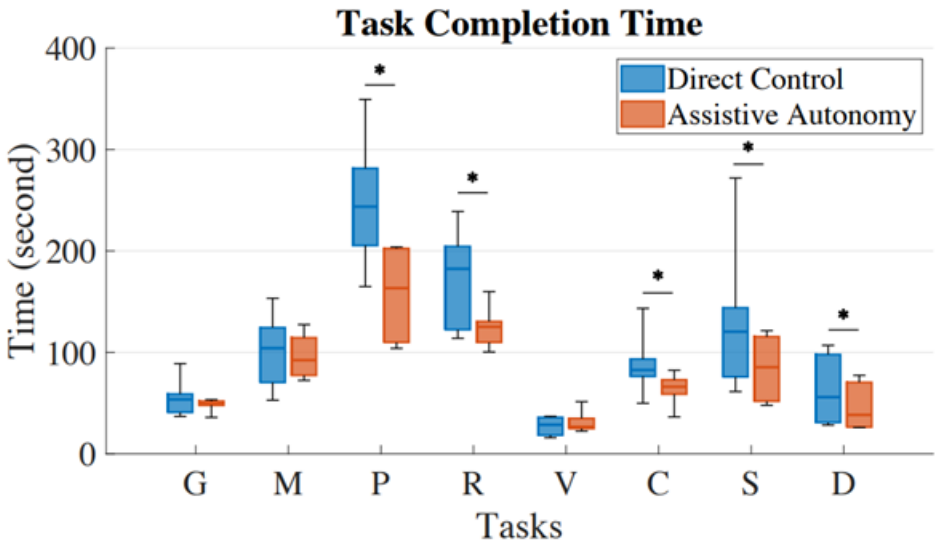
VOCAB: (w/definition)	• Shared autonomy: Control framework combining human guidance with autonomous robot execution. • Fatigue-adaptive shared control: An adaptive system that reduces operator workload by adjusting autonomy based on conditions. • Inverse kinematics: Computational method for determining joint configurations to achieve a desired position. • Degrees of freedom (DOF): Number of independent movements available to a manipulator or arm.

	• Proximity method: The chest-arm coordination algorithm where the robot autonomously adjusts the chest near workspace limits. • Scaling method: The control strategy that maps the operator input to the chest and arm motion • ROS: Robot Operating System, an open-source framework for developing software on robots • Unity: A program used for simulating robot motions • Kinematic singularity: Configuration where a manipulator loses certain degrees of freedom or motion becomes undefined.
Cited references to follow up on	R. Ye, W. Xu, H. Fu, R. K. Jenamani, V. Nguyen, C. Lu, K. Dimitropoulou, and T. Bhattacharjee, “Rcare world: A human-centric simulation world for caregiving robots,” in 2022 IEEE/RSJ International Conference on Intelligent Robots and Systems (IROS). IEEE, 2022, pp. 33–40.
Follow-up Questions	How could the hybrid strategies be optimized to use human and robot movements to the fullest?

Article #8 Notes: Surrogate modeling for flow simulations using design variable coded deep learning networks

Source Title	Surrogate modeling for flow simulations using design variable-coded deep learning networks
Source citation (APA Format)	Matai, R. (2025). Surrogate modeling for flow simulations using design variable-coded deep learning networks. *Journal of Engineering and Applied Science*, *72*(1). https://doi.org/10.1186/s44147-025-00634-8
Original URL	https://jeas.springeropen.com/articles/10.1186/s44147-025-00634-8
Source type	Journal Article
Keywords	Deep learning, surrogate modeling, flow simulation
#Tags	#Deep_learning, #CFD, #FlowSim
Summary of key points + notes (include methodology)	This study is about a Design Variable-Coded Multilayer Perceptron (DV-MLP) that predicts flow simulations by using spatial coordinates and design variables in a neural network, avoiding the computational expense of CNNs. The model was trained using backpropagation with regularization, early stopping, and learning rate reduction on RANS CFD data with flow regimes from fully attached to fully separated boundary layers, then tested on unseen geometries to evaluate the models ability to interpolate. Results showed $R^2 > 0.99$ with accurate near-wall behavior predictions including flow separation, though with minor deviations in adverse pressure gradient regions, demonstrating effective generalization within the training data range. The mesh-independent surrogate is significant because it can provide rapid predictions (seconds vs. hours) suitable for design optimization and uncertainty quantification, even though it was limited by its interpolation capabilities in adverse pressure gradients.
Research Question/Problem/ Need	The research objective is to demonstrate that a Design Variable-Coded MLP can model critical near-wall flow behavior for unseen geometries when trained on CFD data.

Important Figures	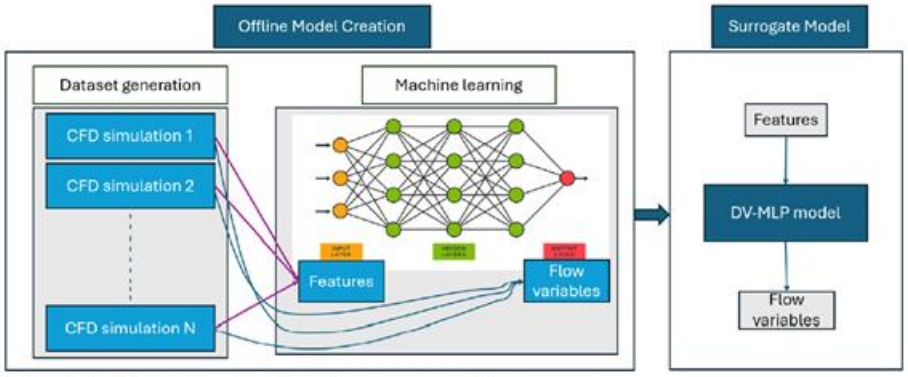 **Fig. 2** Methodology to create and use the surrogate model 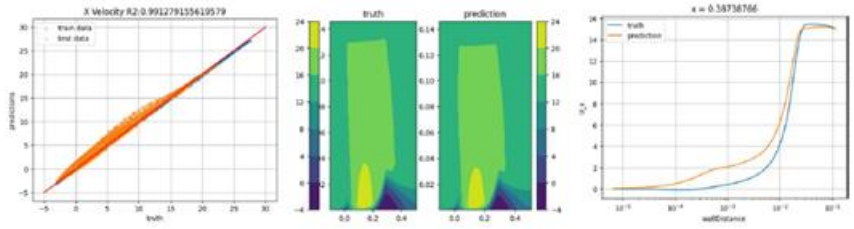 (a) Model performance at $Re_C = 1.73e+5$ (b) x-Velocity Contour at $Re_C = 1.73e+5$ (c) y-Velocity at x = 0.38 at $Re_C = 1.73e+5$ 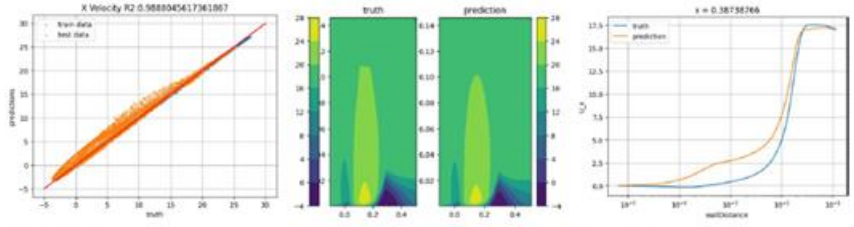 (d) Model performance at $Re_C = 1.97e+5$ (e) x-Velocity Contour at $Re_C = 1.97e+5$ (f) y-Velocity at x = 0.38 at $Re_C = 1.97e+5$ 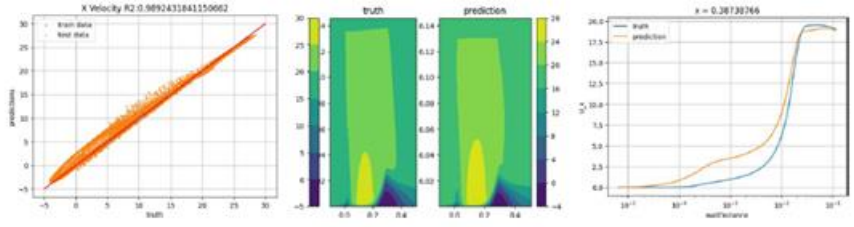 (g) Model performance at $Re_C = 2.21e+5$ (h) x-Velocity Contour at $Re_C = 2.21e+5$ (i) y-Velocity at x = 0.38 at $Re_C = 2.21e+5$ **Fig. 12** MLP Performance when h42 is test dataset
VOCAB: (w/definition)	• Surrogate model: A simpler and faster ML model that is trained to mimic the behavior of a computationally expensive or complex system without performing the computations and just predicting it instead

	• MLP (Multilayer Perceptron): A feedforward neural network with multiple layers of nodes including an input stage, hidden stages, and an output stage to extract patterns in data through multiple layers of analysis • RANS: A CFD method that solved time averaged versions of the Navier Stokes equations which decreases the computational load of running such simulations • Backpropagation: A training algorithm that adjusts neural network weights and biases by calculating gradients of a loss function with respect to each parameter • Regularization: Techniques applied to a neural network's weights and biases such as kernel and bias regularization to prevent overfitting and improve model generalization • Learning rate reduction: A training technique that dynamically decreases the step size of weight updates when a loss plateaus which allows the parameters of a neural network to be finetuned • MinMaxScaler: A data preprocessing technique that normalizes input features into a fixed range to stabilize training • Interpolation: Predicting values within the range of training date • Extrapolation: Predicting values outside the range of the training date, and this is where models 28sually underperform
Cited references to follow up on	Zhao Y, Akolekar HD, Weatheritt J, Michelassi V, Sandberg RD (2020) Rans turbulence model development using cfddriven machine learning. J Comput Phys 411:109413 Zhao L, Zhou Q, Li M, Wang Z (2024) Evaluating different cfd surrogate modelling approaches for fast and accurate indoor environment simulation. J Build Eng 95:110221
Follow-up Questions	How can this method of using ML surrogates be further simplified to provide real time classification with low compute? What methods can be used to allow for turbulent flow to be modeled with an ML surrogate where the flow becomes 3D?

Article #9 Notes: Dynamic Stall Control Using Deployable Leading-Edge Vortex Generators

Source Title	Dynamic Stall Control Using Deployable Leading-Edge Vortex Generators
Source citation (APA Format)	Le Pape, A., Costes, M., Richez, F., Joubert, G., David, F., & Deluc, J.-M. (2012). Dynamic stall control using deployable leading-edge vortex generators. *AIAA Journal*, *50*(10), 2135–2145. https://doi.org/10.2514/1.j051452
Original URL	https://arc-aiaa-org.ezpv7-web-p-u01.wpi.edu/doi/10.2514/1.J051452
Source type	Journal Article
Keywords	Stall control, vortex generators, deployable
#Tags	#Flow_control, #Aerodynamic, #Real_World_Testing
Summary of key points + notes (include methodology)	The researchers designed and tested deployable vortex generators (DVGs) on an airfoil in a wind tunnel, using a row of small retractable blades at the leading edge that could be deployed at various heights and different phases during the airfoil's oscillation cycle. Numerical simulations were used to understand the vortex generation. The deployable vortex generator system consisted of multiple vortex generators spanwise, actuated by dual hydraulic linear motors with position sensors for precise height control, and each blade was shaped to conform perfectly to the airfoil leading edge when retracted and featuring structural stiffness for high-frequency deployment suitable for helicopter rotor applications. The most effective dynamic stall control was achieved with DVGs deployed at moderate heights just before maximum angle of attack with only partial duty cycle, demonstrating that properly timed deployment could achieve reduction in drag while preserving maximum lift, with the key mechanism being prevention of leading-edge separation and dynamic stall vortex formation. The DVGs successfully reduced negative pitching moment peaks and delayed static stall, but introduced significant drag penalties at low angles of attack when deployed, showing the necessity of active rather than passive vortex generators to avoid performance penalties during non-stalled conditions, with the retracted configuration producing a slight additional drag compared to a clean airfoil.

Research Question/Problem/ Need	Can deployable leading edge vortex generators delay stall and alleviate its conditions on helicopter rotor blades by reducing negative pitching moments?
Important Figures	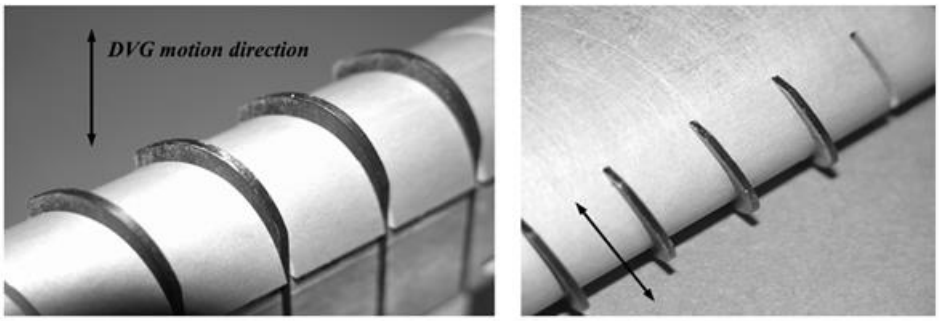 Fig. 3 OA209 model leading edge with close view of the deployable vortex generators (DVGs). 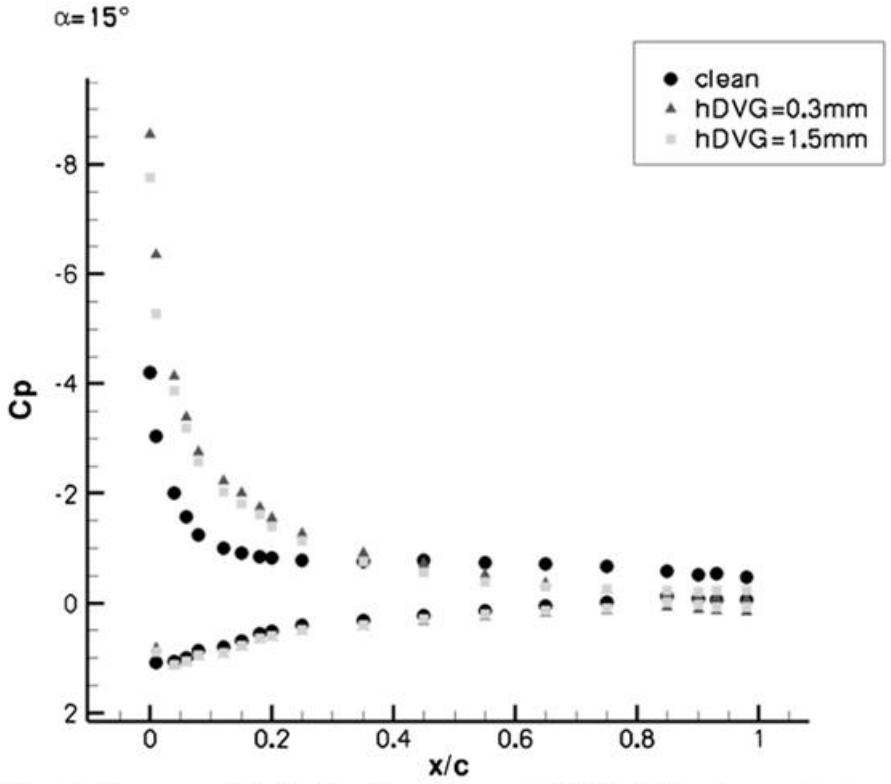 Fig. 6 Pressure distribution for different DVG heights at $\alpha = 15$ deg.
VOCAB: (w/definition)	• Dynamic stall: When the flow separates on moving airfoils that could be oscillating or pitching and produces stronger effects than static stall • Pitching moment: A rotational aerodynamic force about the airfoil's reference point that tries to pitch the airfoil nose-up or nose down

	• Hysteresis loop: The difference in aerodynamic force coefficients such as lift, drag, and moment between the uptake and downstroke portions of an oscillation • Leading-Edge Separation: Flow detachment occurring at or near the airfoil leading edge, typically resulting in sharp, severe stall with complete loss of suction peak and aerodynamic performance degradation. • Trailing-Edge Separation: Flow detachment beginning at the airfoil trailing edge and progressing forward with increasing angle of attack, resulting in gradual, progressive stall with less severe performance penalties than leading-edge separation. • Boundary layer: A thin layer of fluid where viscous effects are high and velocity is affected by the free stream value
Cited references to follow up on	Osborn, R., Kota, S., Hetrick, J., Geister, D., Tilmann, C., and Joo, J., "Active Flow Control Using High-Frequency Compliant Structures," Journal of Aircraft, Vol. 41, No. 3, May–June 2004, pp. 603–609. Doi:10.2514/1.111 Lin, J., "Review of Research on Low-Profile Vortex Generators to Control Boundary-LayerSeparation," Progress in Aerospace Sciences, Vol. 38, Nos. 4–5, 2002, pp. 389–420.
Follow-up Questions	What are the key differences between the control logic in deployable vortex generators for a helicopter blade and an airplane wing? Why did the authors choose to focus on alleviating stall rather than delaying stall or decreasing drag?

Article #10 Notes: Closed-Loop Flow Separation Control Using the Deep Q Network over Airfoil

Source Title	Closed-Loop Flow Separation Control Using the Deep Q Network over Airfoil
Source citation (APA Format)	Shimomura, S., Sekimoto, S., Oyama, A., Fujii, K., & Nishida, H. (2020). Closed-loop flow separation control using the Deep Q network over airfoil. *AIAA Journal*, *58*(10), 4260–4270. https://doi.org/10.2514/1.j059447
Original URL	https://arc-aiaa-org.ezpv7-web-p-u01.wpi.edu/doi/epdf/10.2514/1.J059447
Source type	Journal Article
Keywords	Flow separation, Deep Q Network
#Tags	#Flowcontrol, #CFD, #DeepLearning
Summary of key points + notes (include methodology)	Traditional plasma actuator flow control uses fixed burst frequencies that cannot adapt to changing conditions, and this study tests whether deep reinforcement learning can discover superior adaptive strategies through real-time response to flow measurements and sensor inputs. A Deep Q-Network was trained with hundreds of wind tunnel experiments to find optimal plasma actuator frequencies based on pressure sensor data, and the sensor was used for learning to control flow separation on an airfoil at different stall conditions. At moderate separation, the system matched the best conventional control methods, while at severe separation where fixed-frequency control was ineffective, and the deep learning discovered a novel intermittent on-off cycling strategy achieving 3-4× longer flow attachment.
Research Question/Problem/ Need	Can deep reinforcement learning trained on CFD and wind tunnel test data be used to predict transient flow behavior on airfoils by taking in sensor data.

Important Figures	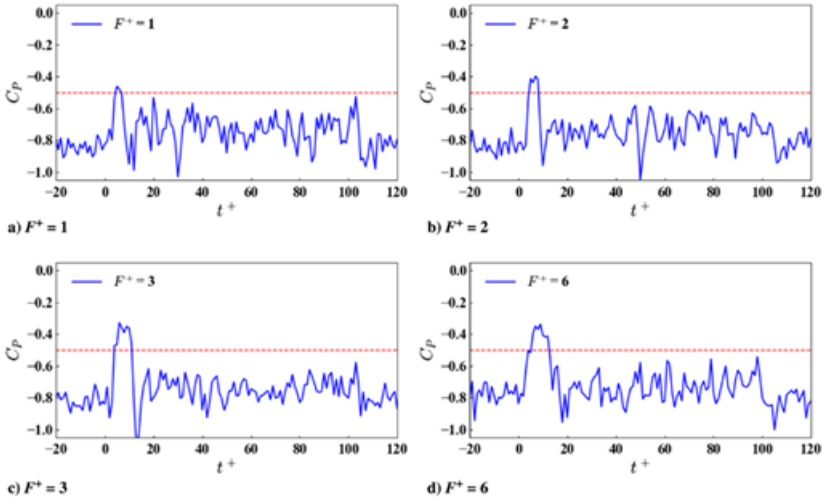 a) $F^+ = 1$ b) $F^+ = 2$ c) $F^+ = 3$ d) $F^+ = 6$ **Fig. 15 Time series of pressure coefficient of the training edge at the angle of attack of 15 deg; the plasma actuator is turned on from 0.0 to 1.0 s.** 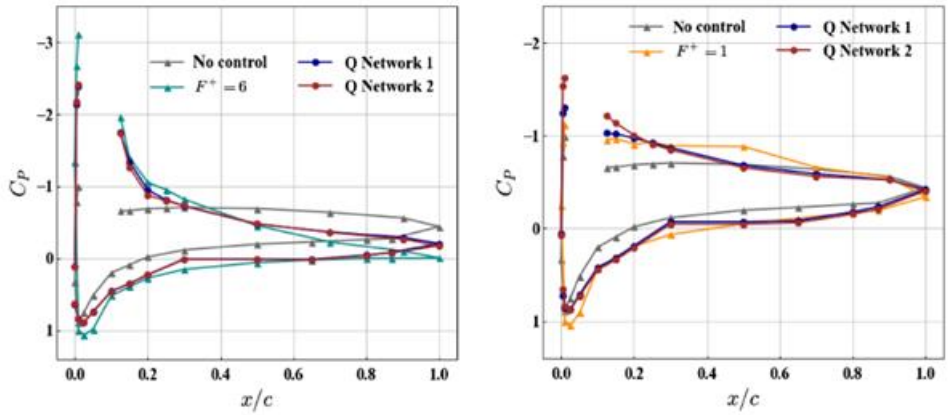 a) C_P distribution at the angle of attack of 12 degrees b) C_P distribution at the angle of attack of 15 degrees **Fig. 12 C_P distribution obtained in the fixed F^+ and DQN control.**
VOCAB: (w/definition)	• Deep Q-Network (DQN): A reinforcement learning algorithm using neural networks to learn optimal decisions through trial-and-error • Dielectric Barrier Discharge Plasma Actuator (DBDPA): A flow control device that uses high voltage to create plasma, generating small jets to inject momentum into the boundary layer. • Burst Frequency: Nondimensional rate at which the actuator cycles on and off, determining the timing pattern of flow control interventions. • Flow Separation: When airflow detaches from the airfoil surface at high angles, causing dramatic loss of lift and increased drag, and it is also known as airfoil stall. • Experience Replay: A training method that stores past experiences and randomly samples them during learning, preventing the network from overfitting to sequential patterns.

	• Pressure Coefficient: Nondimensional measure of surface pressure; values near zero indicate healthy attached flow while large negative values indicate separated flow. • ε-greedy Strategy: An exploration approach for AI models, balancing random action selection (trying new things) with choosing known good actions (exploiting learned knowledge) during training.
Cited references to follow up on	Brunton, S. L., and Noack, B. R., "Closed-Loop Turbulence Control:Progress and Challenges," Applied Mechanics Reviews, Vol. 67, No. 5,2015, Paper 050801. Seidel, J., Fagley, C., and McLaughlin, T., "Feedback Flow Control:A Heuristic Approach," AIAA Journal, Vol. 56, No. 10, 2018, pp. 3825–3834.
Follow-up Questions	How does the accuracy of the deep reinforcement learning model change as Re changes or different airfoils are used? How can the output from the AI model be used to actuate a motor, and what changes would need to be made before actuation can occur.

Article #11 Notes: Review of research on low-profile vortex generators to control boundary-layer separation

Source Title	Review of research on low-profile vortex generators to control boundary-layer separation
Source citation (APA Format)	Lin, J. C. (2002b). Review of research on low-profile vortex generators to control boundary-layer separation. *Progress in Aerospace Sciences*, *38*(4–5), 389–420. https://doi.org/10.1016/s0376-0421(02)00010-6
Original URL	https://doi-org.ezpv7-web-p-u01.wpi.edu/10.1016/S0376-0421(02)00010-6
Source type	Journal article
Keywords	Vortex generator, separation
#Tags	#FlowControl, #VortexGenerators, #BoundaryLayerSeparation
Summary of key points + notes (include methodology)	Low profile vortex generators are designed as flow control devices with heights between 10% and 50% of the local boundary layer thickness, producing far lower drag compared to conventional vortex generators. They have effectiveness that depends heavily on placement upstream of separation points, with critical configuration and sizing details like counter-rotating, co-rotating, and wedge types each exhibiting distinct strengths for various flow scenarios. Effective boundary layer control depends on parameters such as shape, chord length, spanwise spacing, and precise placement. The lower device heights of low profile vortex generators are useful for minimizing parasitic drag .Proper spacing between individual vanes further reduces mutual vortex interference and optimizes vortex decay. CFD and wind tunnel studies demonstrate that excessive device height, poor spacing, or improper placement can increase separation and inefficient drag. For specific applications ranging from low-Reynolds airfoils to high-lift systems and transonic flows, performance gains require tailored choices like wishbone or ramp VGs with targeted h/δ ratios and incidence angles, with the optimum device height typically ranging from 0.1 to 0.5 times boundary layer thickness. Computational methods like effector grids can cut simulation costs by 70% while achieving qualitative accuracy, but must be used alongside experimental data for validation. Having successful low profile vortex generators involves matching configuration type, device height, and placement to the boundary layer and flow objectives, and it

	involves balancing drag reduction against potential adverse wake or separation when control parameters are not correctly chosen.
Research Question/Problem/ Need	What are the effects of low profile vortex generators across a variety of airfoils and flow regimes in controlling boundary layer separation?

Important Figures	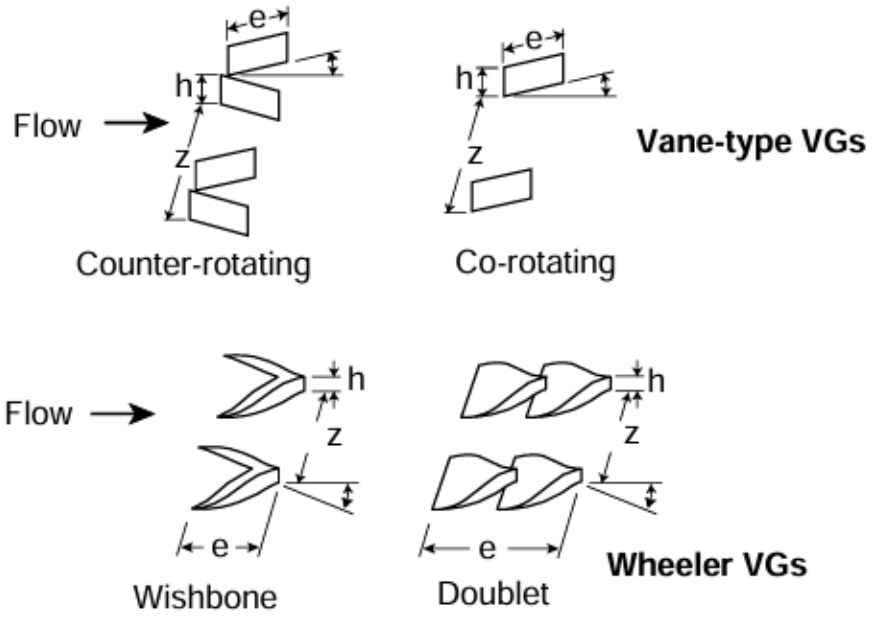 (b) VG geometry and device parameters.

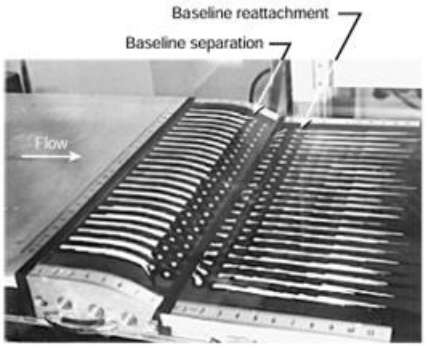

(a) Baseline (VG off) case.

(b) 0.8δ-high vane-type counter-rotating VGs at 6 h upstream of baseline separation.

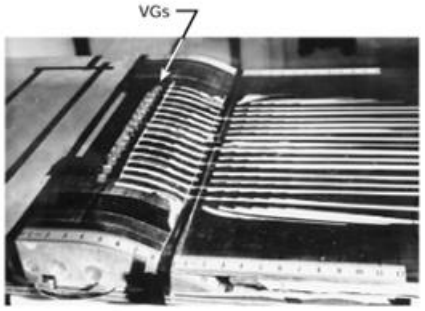

(c) 0.2δ-high vane-type counter-rotating VGs at 10 h upstream of baseline separation.

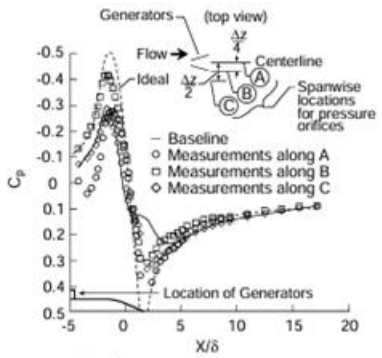

(a) 0.8δ-high vane-type counter-rotating VGs at 6 h upstream of baseline separation.

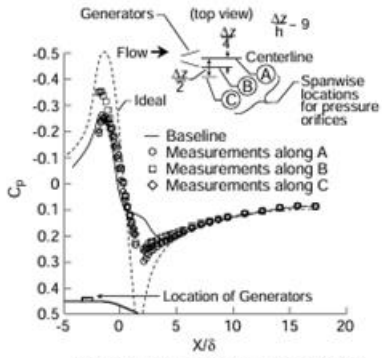

(b) 0.2δ-high vane-type counter-rotating VGs at 10 h upstream of baseline separation.

Fig. 3. Effect of VGs on spanwise variation of the streamwise pressure distributions [16].

vortices are relative weak in the region of separation (after covering 52h in an adverse pressure gradient), they still maintain the ability to attenuate the separated flow region.

Jenkins et al. [17] present another recent experiment carried out at the NASA Langley Research Center 15-in Low-Turbulence Wind Tunnel at $U_\infty = 140$ ft/s. The flow-control devices are evaluated over a backward-facing ramp that is dominated with 3D separated flow formed by two large juncture vortices—one over each side-corner of the ramp [17]. These two large vortical

<table>
<tr>
<td></td>
<td>
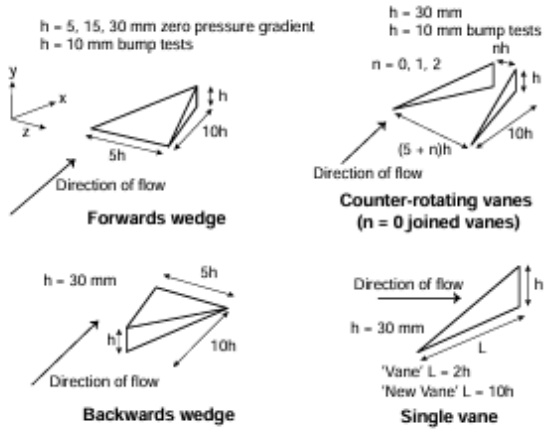

(a) Geometry of SBVGs.

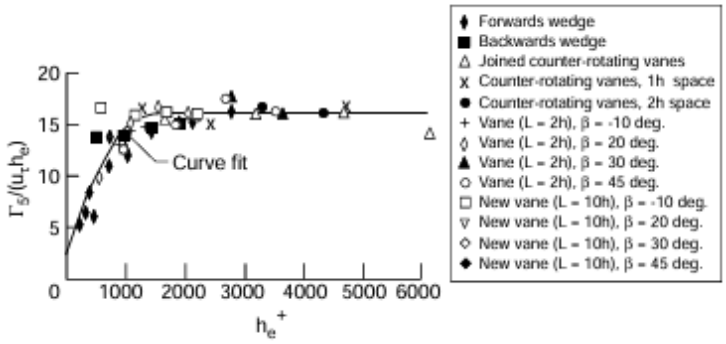

(b) Non-dimensional circulation based on effective height versus non-dimensional effective height.

Fig. 9. Device geometry and correlation of vortex strength against device Reynolds number [20].

</td>
</tr>
<tr>
<td>VOCAB: (w/definition)</td>
<td>

Streamwise vorticity: The rotational motion of a fluid about an axis aligned with the primary flow direction, generated by vortex generators to transfer high momentum fluid from the outer flow toward the wall
Circulation is a quantitative measure of vortex strength defined as the line integral of velocity around a closed path that contains the vortex. Higher circulation values mean stronger vortices
Boundary Layer displacement thickness: The distance by which the external flow is displaces outward due to the boundary layer. It represents the reduction in mass flow caused by the velocity deficit within the boundary layer
Boundary layer momentum thickness: This quantifies the deficit in momentum flux within the boundary layer compared to inviscid flow.
Laminar separation bubble: This is what is formed when a laminar boundary layer separates due to adverse pressure gradients, and it

</td>
</tr>
</table>

	also forms when turbulent flows are transitioned to in the shear layer, and then the flow reattaches as turbulent flow • Shock induced separation: This occur in transonic and supersonic flow when a shockwave creates a sudden adverse pressure gradient that causes the boundary layer to separate • Vortex decay: The gradual reduction in vortex strength and circulation as a streamwise vortex travels downstream • Effector model grid: A simplified CFD method that uses boundary conditions to represent vortex generator effects rather than fully computing on the device geometry. It can cut compute by 70% • Adverse pressure gradient: An adverse pressure gradient is a condition where the static pressure increases in the direction of flow, which causes the near-wall fluid to decelerate and can lead to boundary-layer separation if the low-momentum fluid cannot overcome the rising pressure
Cited references to follow up on	None
Follow-up Questions	• What are key differences in the designs of vortex generators for high vs low Re and how should these differences be taken into account for implementation? • How impactful is the parasitic drag caused by static vortex generators in aircraft that could suffer from shock induced separation?

Article #12 Notes: A review of the use of vortex generators for mitigating shock-induced separation

Source Title	A review of the use of vortex generators for mitigating shock-induced separation
Source citation (APA Format)	Titchener, N., & Babinsky, H. (2015a). A review of the use of vortex generators for mitigating shock-induced separation. *Shock Waves*, *25*(5), 473–494. https://doi.org/10.1007/s00193-015-0551-x
Original URL	https://wpi.primo.exlibrisgroup.com/permalink/01WPI_INST/1pchs3f/cdi_crossref_citationtrail_10_1007_s00193_015_0551_x
Source type	Journal Article
Keywords	Vortex generator, separation, shock
#Tags	#TransonicFlow, #ShockInducedSeparation, #Aerodynamic Efficiency
Summary of key points + notes (include methodology)	This article explores how vortex generators can mitigate shock-induced boundary layer. The study found that low-profile vortex generators with heights between 0.2 and 0.5 times the boundary layer thickness work best for transonic applications, with counter-rotating arrays spaced at D/d ≥ 4 consistently outperforming other configurations. Vane or swept-vane shapes were known to perform better than vortex generators with ramp shapes. Many studies showed clear aerodynamic benefits in transonic flows such as improved lift-to-drag ratios and pressure recovery, with optimal VG placement at 15-30h upstream of the separation point. Vortex generators in purely subsonic applications had little benefits. The review includes critical research gaps including how the device drag penalty of vortex generators is hardly ever measured, three-dimensional corner flow effects that can negate benefits are present, and there is an unknown lower limit on vortex generator height where vorticity production becomes insufficient. This article supports my project idea of an adaptive deployable vortex generator systems because it could address the limitation of passive devices by retracting when separation risk is low to eliminate cruise drag penalties.
Research Question/P	What are the effects of vortex generators on shock induced boundary layer separation?

roblem/ Need	
Important Figures	

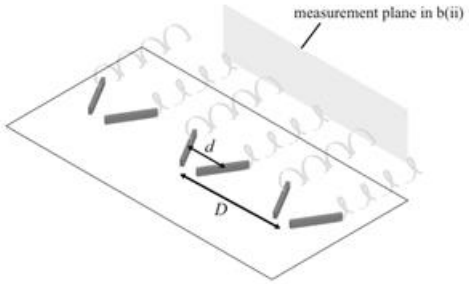

(i) Schematic drawing showing VG variables

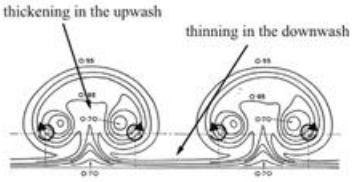

(ii) Example Pitot pressure contours in a plane normal to the vortex core

(b) Counter-rotating vortex generators

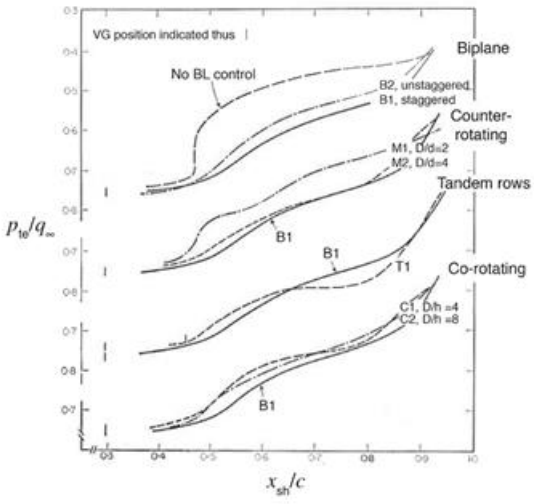

(d)

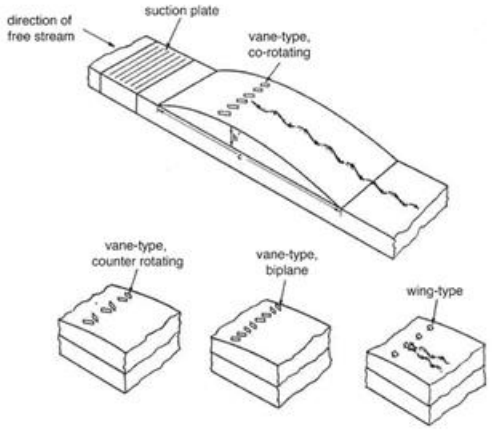

(a)

	h/c	D/h	D/d	l/h	α (deg)
Co-rotating					
C1	0.01	4	-	4	20
C2	0.01	8	-	4	20
C3	0.02	4	-	4	25
C4	0.012	5	-	4	25
C5	0.01	4	-	triangular	12
Counter-rotating					
M1	0.01	5	2	2.5	15
M2	0.01	10	4	2.5	15
M3	0.01	5	4	1.25	15
M4	0.01	6.3	2.7	3.6	15
M5	0.004	6.3	2.7	3.6	15
Bi-plane					
B1	0.01	11.25	4.5	2.5	15, 20
B2	0.01	10	4	2.5	15
B3	0.01	5	4	1.6	15
Tandem row					
T1 row 1	0.02	8	4	wing-type (square)	15
T1 row 2	0.01	16	4	4	20

(b)

VOCAB: (w/definition)	• Vortex liftoff: The phenomenon when streamwise vortices move away from the surface in the direction normal to the wall, and this reduces the effectiveness of vortex generators as the vortices become less powerful and energized • Shock-Boundary Layer Interaction: When a shock interacts with the boundary layer and creates an adverse pressure gradient • Upwash region: The area behind vortex generators where low-stagnation pressure exists • Downwash region: The area between diverging counter rotating vortex generators where the high momentum fluid is transferred to the boundary layer • Loss redistribution: When vortex generators reduce separation in the center-span region but that improvement increases the effective flow area, which causes uncontrolled corner regions to experience higher adverse pressure gradients • Device drag: The parasitic drag penalty of vortex generators when they are not preventing stall • Separation topology: The three-dimensional structure and organization of separated flow regions. This is especially relevant when quantifying vortex effects and spanwise effects
Cited references to follow up on	Gould, D.G.: The use of vortex generators to delay boundary layer separation. Technical Report, Unpublished NAE (Canada) Laboratory Rao, D., Kariya, T.: Boundary-Layer Submerged VortexGenerators for Turbulent Flow Separation Control—An Exploratory Study, AIAA-88-3546-CP (1988)
Follow-up Questions	Are there any frameworks to quantify the effects of small geometric changes in the configurations of vortex generators? How do the unsteady dynamics of shock induced separation and fluctuations in boundary layer behavior affect the time needed for vortex generator effectiveness? How does device drag increase with parameters that define a vortex generator's geometry?

Article #13 Notes: Deployable vortex generators for low Reynolds numbers applications powered by cephalopods inspired artificial muscles

Source Title	Deployable vortex generators for low Reynolds numbers applications powered by cephalopods inspired artificial muscles
Source citation (APA Format)	Mamman, R., Kotak, P., Weerakkody, T., Johnson, T., Krebill, A., Buchholz, J., & Lamuta, C. (2023b). Deployable vortex generators for low Reynolds numbers applications powered by cephalopods inspired artificial muscles. *iScience*, *26*(12), 108369. https://doi.org/10.1016/j.isci.2023.108369
Original URL	https://wpi.primo.exlibrisgroup.com/permalink/01WPI_INST/1pchs3f/cdi_doaj_primary_oai_doaj_org_article_c0c7cc2b2e1a4a539e39ebed706d6c24
Source type	Journal Article
Keywords	Deployable, vortex generator, low Reynolds number
#Tags	#FlowControl, #AerodynamicEfficiency
Summary of key points + notes (include methodology)	This article is about developing a system of deployable vortex generators for low Reynolds number applications where the actuation of the vortex generators is done by twisted spiral artificial muscles (TSAMs). All of the testing for the plain airfoil, the airfoil with static vortex generators, and the deployable vortex generators were done at Re of 100k and 140k using a low Re airfoil, and only wind tunnel testing was done with no simulation. There was no systematic method of finding vortex generator configurations, so the researchers did not use optimal VG placement, but they instead used trial-and-error to test over 20 configurations, and VGs were tested to try and match static with deployable. The deployable vortex generators to match each static configuration, showing how there is potential for further development of deployable vortex generator systems. The TSAMs are very cheap and provide 2000% strain with low voltage, but they are very sensitive to temperature and have high latency, making them a bad choice for actuators on a real aircraft. Wind tunnel testing with splitter plates was done to simulate 2D flow, and angle of attack was varied and Reynolds number was varied. The control of the system was done with an L1 adaptive controller using temperature feedback to prevent thermal degradation, but the deployable VGs only matched to different preset configurations and did not

	adapt to choose the truly optimal configuration that could have been in between the predetermined ones. The authors did not provide data about drag, pressure, or flow fields, they included only lift, which means there's no way to evaluate aerodynamic efficiency of their system.
Research Question/ Problem/ Need	Can deployable vortex generators, actuated by twisted spiral artificial muscles, match the performance of static vortex generators at low Reynolds numbers?
Important Figures	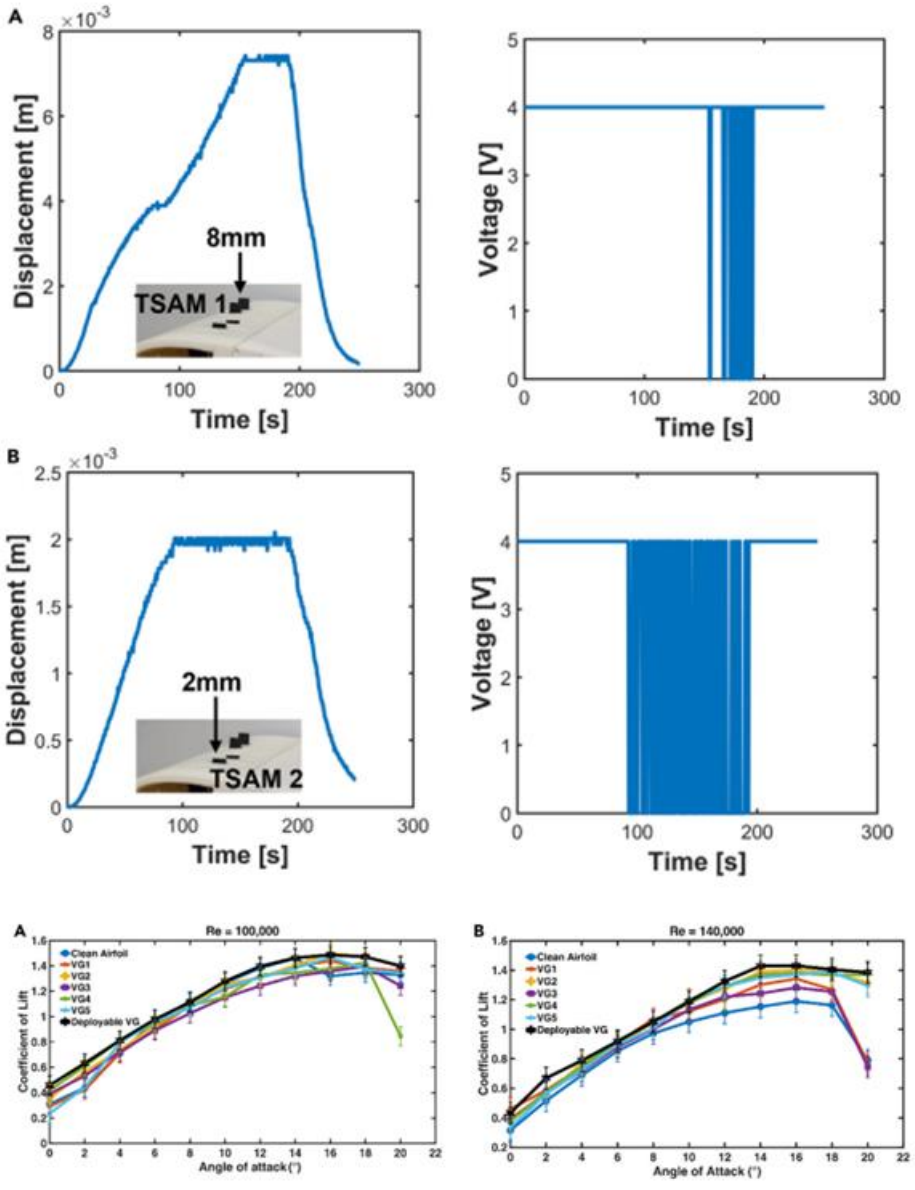

VOCAB: (w/definition)	• L1 Adaptive Controller: A control algorithm that uses feedback to improve precision of output • Thermoresistor: A temperature sensor that changes in resistance with temperature • Splitter Plate: A flat barrier installed parallel to the wing in wind tunnel experiments to simulate quasi-2D flow which prevents tip vortices • Lookup Table: A control strategy used in the study where the deployable vortex generators were actuated to heights accordingly with predetermined values • Spanwise Spacing: The distance between adjacent vortex generators along the wing span
Cited references to follow up on	Kirk, T.M., and Yarusevych, S. (2017). Vortex shedding within laminar separation bubbles forming over an airfoil. Exp. Fluids 58, 43. https://doi.org/10.1007/s00348-017-2308-z Sørensen, N.N., Zahle, F., Bak, C., and Vronsky, T. (2014). Prediction of the effect of vortex generators on airfoil performance. J. Phys. Conf. Ser. 524, 012019. https://doi. Org/10.1088/1742-6596/524/1/012019
Follow-up Questions	How would the control architecture need to change in order to create adaptive control mapped to every possible set of inputs? How would the conclusions of the efficiency of the system change when device drag is accounted for?

Article #14 Notes: CNN based flow control device modelling on aerodynamic airfoils

Source Title	CNN based flow control device modelling on aerodynamic airfoils
Source citation (APA Format)	Portal-Porras, K., Fernandez-Gamiz, U., Zulueta, E., Ballesteros-Coll, A., & Zulueta, A. (2022). CNN-based flow control device modelling on aerodynamic airfoils. *Scientific Reports*, *12*(1). https://doi.org/10.1038/s41598-022-12157-w
Original URL	https://doaj.org/article/f123be3fbfb44bd8a5eb55889589d744
Source type	Journal Article
Keywords	CNN, flow control, airfoil
#Tags	
Summary of key points + notes (include methodology)	• This article is about evaluating the feasibility of using deep learning (CNNs) to predict flow fields and aerodynamic coefficients for airfoils equipped with flow control devices (Gurney flaps and rotating microtabs) as a faster alternative to CFD. • Boundary conditions for the CFD training data included a no-slip condition on the airfoil surface and a freestream velocity of 30 m/s, with the domain defined by an O-mesh of radius 32c (32 m) to avoid boundary effects. • The Re of this simulation was 2 × 10^6, representing a turbulent flow regime typical for wind turbine airfoils. • The domain was a 2D cross-section of a DU91W(2)250 airfoil, a profile widely used in horizontal axis wind turbines (HAWTs). • Gurney flaps were tested with lengths of 0.25% to 2% of chord, and rotating microtabs with lengths of 1%, 1.5%, and 2% of chord. • Angles of attack ranging from 0 to 9 were tested for Gurney flaps and the clean airfoil, and 0 to 5 for microtabs. • Only 2D simulations were conducted, as the study focused on cross-sectional aerodynamic performance rather than 3D vortex dynamics. • Flow control devices were implemented using the cell-set meshing technique, where the geometry is defined on an existing mesh by splitting cells into a new region and assigning wall conditions, rather than regenerating the mesh and fully resolving it • For turbulence modeling, the RANS-based k-ω SST model was used, combining k-ω for near-wall regions and k-ε for the far field.

	• To collect data for training, 158 CFD simulations were run using Star-CCM+ v2019.1, covering various device geometries, orientations (for microtabs), and angles of attack. • To make the mesh, a structured O-mesh with approximately 207,000 cells was used, with refinement near the airfoil to capture gradients. Low amount of cells • Meshes were validated against experimental data from the Delft University Low Speed Wind Tunnel and checked for convergence using the General Richardson Extrapolation method on the lift-to-drag ratio. • For mesh independence, three mesh densities (fine: ~207k, medium: ~103k, coarse: ~52k cells) were tested, and the fine mesh was selected as the solution fell within the range of convergence. • The CNN input consisted of four 128 × 256 layers. two binary layers representing the airfoil and device geometry (overview and close-up), and two layers representing the x and y velocity components to help the network identify the angle of attack. • Two distinct CNN architectures were used, a U-Net architecture for predicting velocity and pressure fields, and a standard CNN with a fully connected layer for predicting scalar aerodynamic coefficients (Cl and Cd). • The U-Net architecture is an encoder-decoder network that captures spatial features through convolutions and downsampling, then reconstructs the field through upsampling and concatenation with encoder features. • Results showed the CNN could predict velocity and pressure fields with high accuracy, with the main errors occurring in the complex wake region behind the flow control device. • Aerodynamic coefficient predictions were reliable, with mean relative errors of 0.827% for Cl and 6.17% for Cd, capturing the correct trends for different device configurations. • The CNN approach was significantly faster than CFD, with a speedup of roughly 7,500x for field prediction and 16,000x for coefficient prediction, reducing computational time by four orders of magnitude. • Some limitations include the focus on steady-state RANS data which may not capture unsteady shedding phenomena, and the fact that the model is specific to the trained airfoil profile and flow conditions
Research Question/Problem/ Need	CFD simulations are slow and expensive, so CNNs could be used to predict the effects of flow control devices on airfoils.

Important Figures	

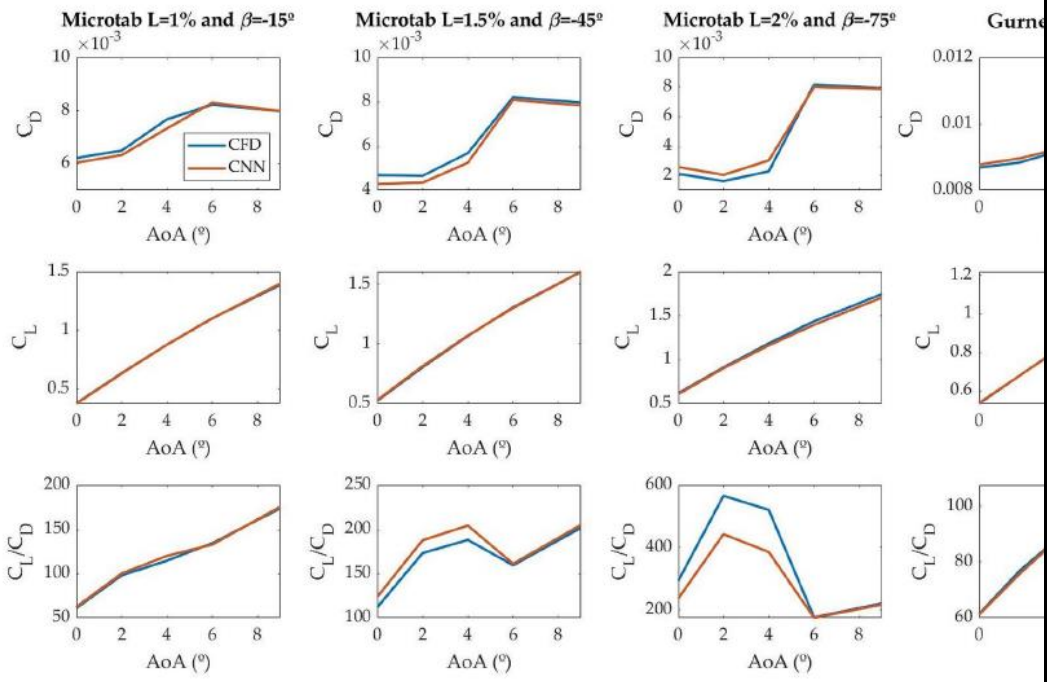

Figure 10. Aerodynamic coefficient comparison of all the tested cases.

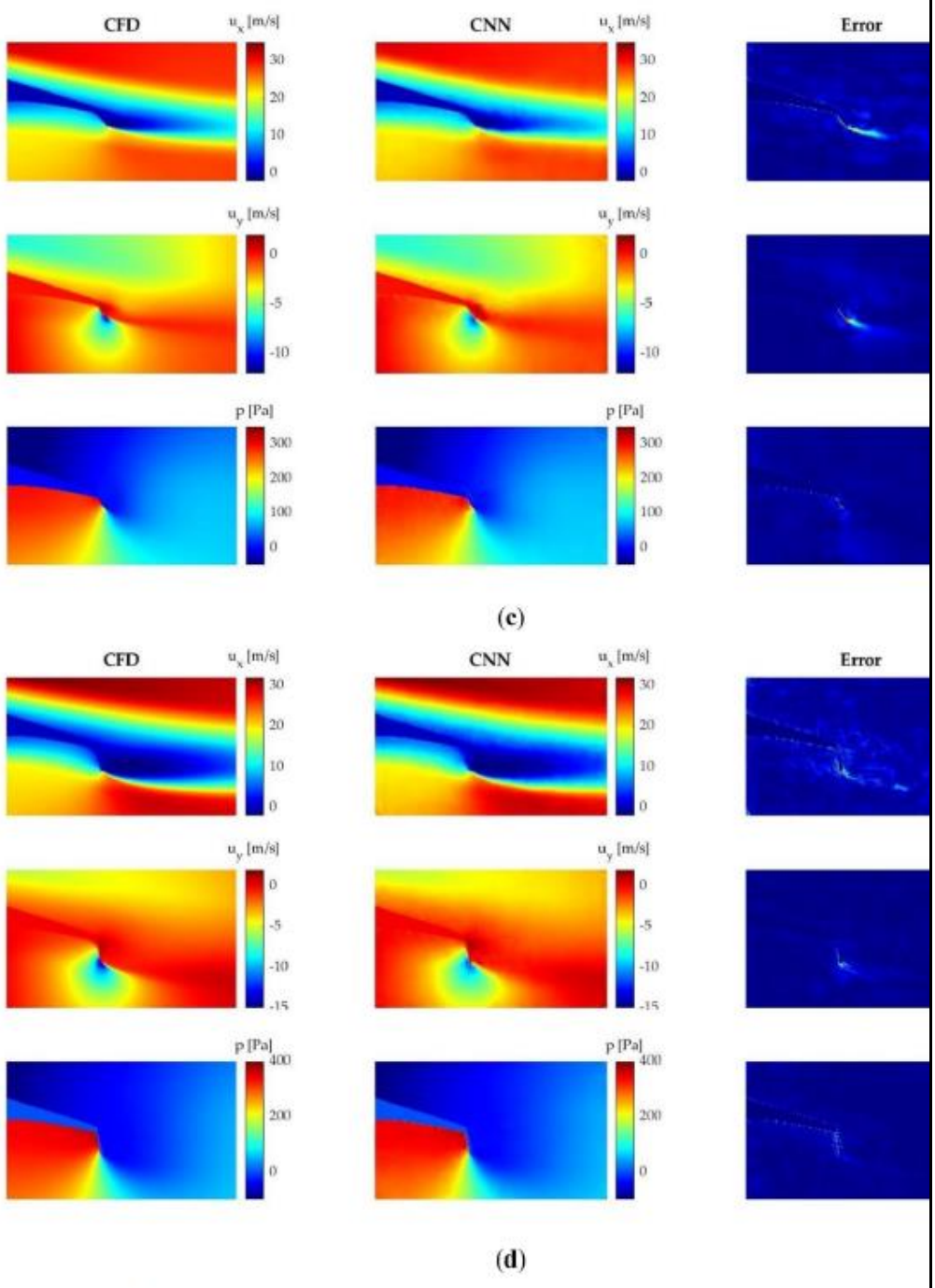

Figure 8. (continued)

VOCAB: (w/definition)	• U-Net architecture: A deep learning network design with an encoder-decoder structure and skip connections, originally made for image segmentation but here used to reconstruct high-resolution flow fields from coarse geometry inputs.

	• Richardson Extrapolation: A numerical method used to estimate the exact solution of a problem by comparing results from meshes of different densities, to verify mesh independence. • O-mesh: A structured mesh topology where grid lines wrap circularly around the airfoil, and this makes high quality cells in the boundary layer and less cells in the far field region • Gurney flap: A small tab projecting perpendicularly from the airfoil pressure side at the trailing edge, used to increase lift • ReLU (Rectified Linear Unit): An activation function used in neural networks that outputs the input directly if positive and zero otherwise, helping the model learn non-linear flow patterns. • Shear Stress Transport (SST) model: A turbulence model that switches between k-ω near the wall and k-ε in the free stream to accurately predict flow separation and boundary layer behavior.
Cited references to follow up on	Ballesteros-Coll, A., Fernandez-Gamiz, U., Aramendia, I., Zulueta, E. & Lopez-Guede, J. M. Computational methods for modelling and optimization of flow control devices. *Energies* **13**, 3710. https:// doi. org/ 10. 3390/ en131 43710 (2020). Portal-Porras, K., Fernandez-Gamiz, U., Ugarte-Anero, A., Zulueta, E. & Zulueta, A. Alternative artificial neural network structures for turbulent flow velocity field prediction. *Mathematics* **2021**, 9. https:// doi. org/ 10. 3390/ math9 161939 (1939). Chen, H., He, L., Qian, W. & Wang, S. Multiple aerodynamic coefficient prediction of airfoils using a convolutional neural network. *Symmetry* **12**, 544. https:// doi. org/ 10. 3390/ sym12 040544 (2020).
Follow-up Questions	How would the cell set method change for trying to get y plus values of less than 1? Would the CNN still be able to approximate accurately in turbulent flow or separating flow?

Article #15 Notes: Testing the Accuracy of the Cell-Set Model Applied on Vane-Type Sub-Boundary Layer Vortex Generators

Source Title	Testing the Accuracy of the Cell-Set Model Applied on Vane-Type Sub-Boundary Layer Vortex Generators
Source citation (APA Format)	Portal-Porras, K., Fernandez-Gamiz, U., Aramendia, I., Teso-Fz-Betoño, D., & Zulueta, E. (2021). Testing the accuracy of the cell-set model applied on Vane-type sub-boundary layer vortex generators. *Processes*, *9*(3), 503. https://doi.org/10.3390/pr9030503
Original URL	https://www.mdpi.com/2227-9717/9/3/503
Source type	Journal Article
Keywords	Vortex Generators
#Tags	
Summary of key points + notes (include methodology)	• This article is about comparing the results of CFD simulations using a mesh generated with the cell-set model as opposed to a fully resolved mesh • Boundary conditions were inlet and outlet for upstream and downstream, no slip walls for VG faces, and symmetry planes for the remaining surfaces to ensure that there is no boundary layer developing on the flow boundaries • The Re of this simulation was 27,000, so mostly laminar, but it could be turbulent • The domain was a flat plate with negligible streamwise pressure to avoid the type of adverse pressure gradient that would be observed in real life • VG heights of .2-1 times the boundary layer height were tested with increments of .2 • Angles of attack of 18 and 25 were tested • Only rectangular VGs were used to keep the results consistent and accurately compare the models • For different VG heights, when it was lower, they were placed in the buffer layer region, which is where viscous effects dominate and the flow is turbulent, and the taller VGs were placed in the outer area • For the angle of attack of 18 degrees, a k-omega SST RANS model was used, and for 25 degrees, SGS model was chosen for LES simulations, as RANS cannot accurately capture high angles of attack

	• To collect data, 12 spanwise planes, perpendicular to the stream were separated by increments of 2 times boundary layer thickness • To make the VG mesh, 11.5 million hexahedral cells were used, and structured meshes were used • Wall distance was set to 1.5*10^-6, aiming for a low y+ • Meshes were heavily refined in the near VG region to capture physical phenomena accurately • To evaluate the mesh, the quality parameters of skewness angle, volume change, and face validity were used. • Skewness angle should be less than 85 degrees, volume change should be less than 0.01, face validity should be 1 • Richardson Extrapolation method was used for mesh independence for RANS meaning a coarse mesh, medium mesh and fine mesh were testing, and the difference between the results was negligible, so the medium was used • For mesh independence for LES, taylor length scale verification was performed • The cell-set model is a meshing technique that generates a desired geometry in a mesh that does not initially contain that geometry • This involves setting the cells by cell id and creating the geometries within the mesh itself, and it results a far coarser mesh for ideally equally-accurate results • Used 56 cores on 45 GB RAM • Q criterion was used to capture vortex shape and size • Peak of vorticity was measured to find vortex path • Vortex strength was calculated using circulation and half-life radius • Wall shear stress was measured on the wake behind the VG trailing edge as a major parameter for quantifying the VG abilities to delay stall • The results were that the cell set model with RANS is reliable until the lowest VG heights, and it is reliable only for tall VGs and completely fails for shorter ones with LES • Some limitations of the study in terms of the rigor of the cell set model are the flat plate setup, the one geometry of VGs being tested, no data on drag, and no field comparisons
Research Question/Problem/ Need	Can the cell-set model reproduce the results RANS and LES simulations of a fully rendered mesh of vortex generators on a flat plate at low Reynolds numbers?

Important Figures	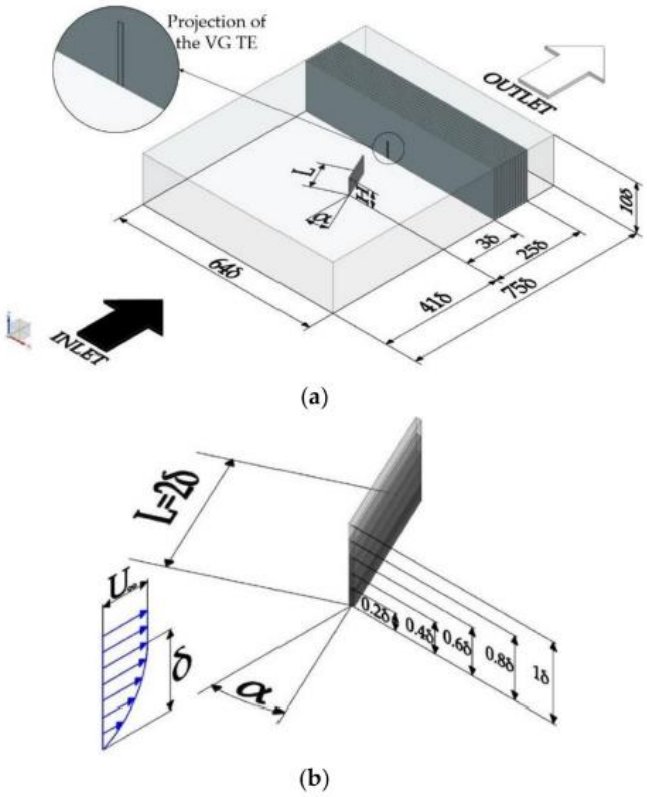 Figure 1. (a) Numerical domain (not to scale). (b) Vortex Generator (VG) parame

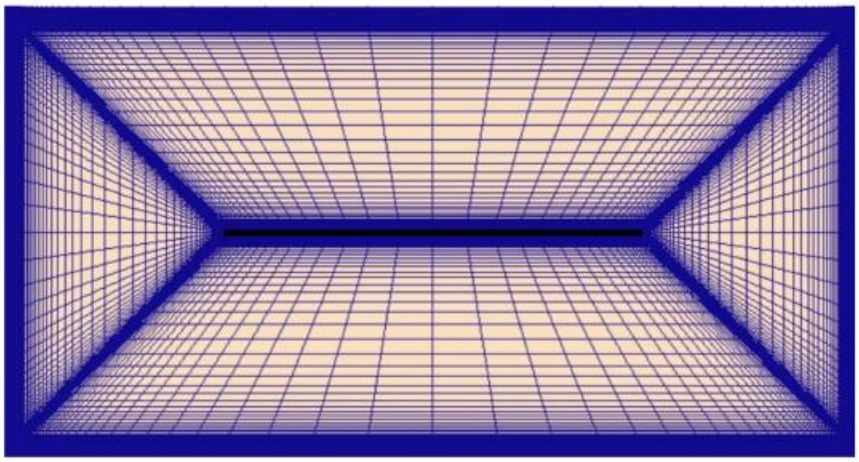

(a)

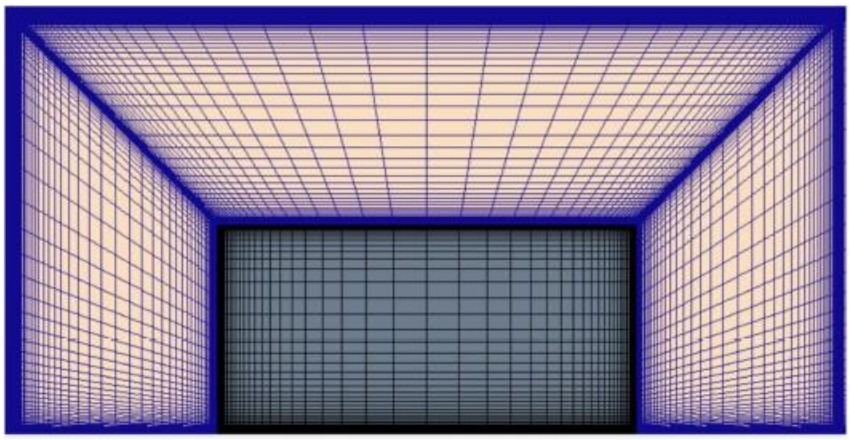

(b)

Figure 2. Refined mesh around the VG for H = 1 δ. (a) Top view and (b) side

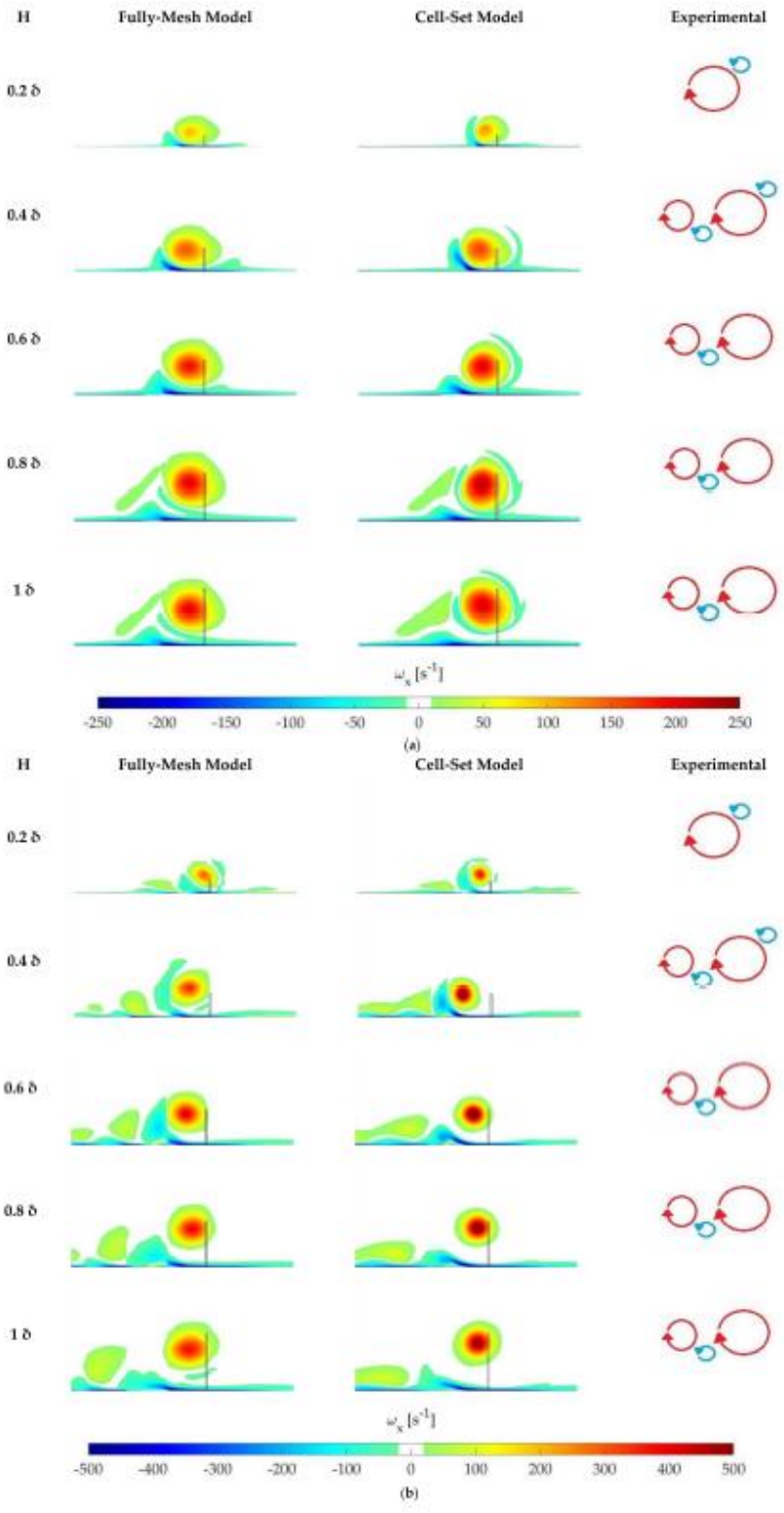

Figure 8. Vortical structures predicted on the wake behind the VG. (**a**) Reynolds-Averaged Navier-Stokes (RANS) ($\alpha = 18°$) and (**b**) Large Eddy Simulation (LES) ($\alpha = 25°$).

VOCAB: (w/definition)	• Cell-set model: A meshing strategy where the VG geometry is created by reassigning existing cells in a base mesh to a wall region instead of explicitly resolving the solid surface with body-fitted cells. • Half-life radius: A vortex size metric defined as the radial distance from the vortex center to the point where local vorticity drops to half of the peak vorticity. • Q-criterion A vortex-identification method based on the second invariant of the velocity gradient tensor, highlighting regions where rotation dominates over strain. • Horseshoe vortex: A vortical structure that wraps around the base of the VG leading edge, splitting into pressure-side and suction-side legs. • Discrete vortex: A secondary vortex formed when the boundary layer lifts and rolls up between the primary vortex and the wall, producing a separate concentrated structure. • Taylor length scale: A turbulence length scale used here to check LES resolution, ensuring the local grid spacing is fine enough to resolve energy-containing eddies in the wake. • Circulation: A scalar measure of vortex strength computed by integrating vorticity over an area (approximated here via peak vorticity and R square), indicating the vortex's mixing capability
Cited references to follow up on	Ibarra-Udaeta, I., Errasti, I., Fernandez-Gamiz, U., Zulueta, E., & Sancho, J. (2019). Computational characterization of a rectangular vortex generator on a flat plate for different vane heights and angles. *Applied Sciences*, *9*(5), 995. https://doi.org/10.3390/app9050995 Allan, B.; Yao, C.-S.; Lin, J. Numerical Simulations of Vortex Generator Vanes and Jets on a Flat Plate. In Proceedings of the 1st Flow Control Conference, St. Louis, MO, USA, 24–26 June 2002; American Institute of Aeronautics and Astronautics: Reston, VA, USA, 2002 Hunt, J.C.R.; Wray, A.A.; Moin, P. Eddies, Stream, and Convergence Zones in Turbulent Flows; Center for Turbulence Research Report CTR-S88; Center for Turbulence Research: Stanford, CA, USA, 1988; pp. 193–208.
Follow-up Questions	Why were measurements of drag not included? How would the methodology and results change if higher Reynolds numbers were tested and the shape was now an airfoil?

Article #16 Notes: Computational Characterization of a Rectangular Vortex Generator on a Flat Plate for Different Vane Heights and Angles

Source Title	Computational Characterization of a Rectangular Vortex Generator on a Flat Plate for Different Vane Heights and Angles
Source citation (APA Format)	Ibarra-Udaeta, I., Errasti, I., Fernandez-Gamiz, U., Zulueta, E., & Sancho, J. (2019a). Computational characterization of a rectangular vortex generator on a flat plate for different vane heights and angles. *Applied Sciences*, *9*(5), 995. https://doi.org/10.3390/app9050995
Original URL	https://www.mdpi.com/2076-3417/9/5/995
Source type	Journal Article
Keywords	vortex generators; half-life radius; flow control; boundary layer; computational fluid dynamics; OpenFOAM
#Tags	
Summary of key points + notes (include methodology)	• This study focuses on the key vortex features formed by single rectangular vortex generators on a flat plate using OpenFOAM, an open-source computational fluid dynamic software, by varying the height of the vortex generator and the incident angle through a parametric study. • Boundary conditions were specified as inflow for the upstream boundary with prescribed undisturbed velocity, outlet for the downstream boundary with assumptions of fully developed velocity profiles, slip for the ceiling boundary of the computational domain as well as the lateral boundaries, and no-slip for both the vane surface and flat plate. • Reynolds number of 27,000 for the calculation of simulation results was determined using the local boundary layer thickness on the vane's leading edge with the freestream velocity of 20 m/s. This is appropriate for the application of the RANS turbulence models for prediction of the primary vortex. • The computational grid consisted of a flat-plate geometry with a zero streamwise pressure gradient with the vane leading edge placed 10.25 m downstream of the inlet with normalized lengths of 64 times width, 10 times height, and 75 times length normalized by the local boundary layer thickness.

	• Six vane heights from 0.2H to 1.2H with an increment of 0.2H were examined, with H being the boundary layer thickness of 0.25 m. This aided in understanding the influence of throwing the through super-boundary-layer generator on sub-boundary layers. • Four incident angles of 10°, 15°, 18°, and 20° were also investigated, which served as a parametric study of vane angle effects on vortex formation and effectiveness of flow control. • Rectangular vane geometry with a fixed length-height ratio of 2:1 was used consistently to separate the individual effects of height and angle independently without altering the geometry. • Short vane span heights result in the vortex shedding process occurring in the buffer region where viscous forces are more dominant, whereas higher vane configurations remove momentum from the external boundary layer, which influences vortex path properties • k-ω Shear-Stress Transport turbulence models were used for RANS simulations at all incident angles, chosen from previous validations that showed better predictions of streamwise peak vorticity and vortex path compared to Spalart-Allmaras models. • Data extraction was carried out for eleven spanwise locations that were normal to the streamwise direction at distances ranging between 1 to 25 times the boundary layer thickness downstream of the vane/trailing edge position. • Structured mesh setups with 12 million hexahedral elements were created for the 0.2H and 0.4H models, as well as 11 million for higher vane heights, using block-based meshing with topology and boundary information conveyed in dictionaries • Wall normal spacing: 1.5 × 10^-6 normalized by boundary layer thickness, with an emphasis on low y+ values for resolution of the viscous sublayer • The refinement of the mesh was focused in the vicinity of the vane to realistically capture vortex formation phenomena and secondary flows in that region with sufficient resolution. • EMesh goodness of fit was determined by using non-orthogonality parameters with values for all non-orthogonal angles set below 70 degrees, with maximum skewness of 3.56 or less • Simulations involved the use of 16 CPU cores with 32 GB RAM that utilized the parallel domain decomposition technique for eight subdomains, with convergence tolerance standards of 10^-5 for residual error in velocity, pressure, and turbulence respectively • Half-life radius was chosen as the key parameter for vortex sizes, which is the distance from the center to where the vorticity is reduced to half of its maximum point, with a Gaussian distribution pattern.

	• Location of the vortex center was determined by peak streamwise vorticity in the spanwise plane perpendicular to the mean flow direction • Vorticity strength was determined by measuring peak vorticity values regardless of vortex size. • Circulation was determined at 5 boundary layer thicknesses downstream of the peak vorticity and half-life radius by using the normalized relationship equation for vortex strength. • Wall shear stress on the flat plate surface downstream of the vane trailing edge was measured as an important performance metric related with boundary layer reattachment and separation control abilities. • Findings indicate that the vortex core grows consistently downstream, strongly related to vane height, with the 0.6H configuration reporting the maximum value of wall shear stress for all incident angles investigated • The vane heights of 0.4H and 0.6H for 18° and 20° incident angles showed the best combined effectiveness in vortex core strength and wall shear stress production, signifying an effective design range for separation control purposes • Vortex lateral trajectory was strongly dependent on incident angle and vane height with increasing deviation for higher vane heights, whereas vertical trajectory was almost independent except for 0.2H, which showed ascent likely caused by dominating viscous interactions at the wall. • It is limited by the geometry of flat plates at a Reynolds number since it is not directly applicable at curved airfoil surfaces or at higher Reynolds numbers in the context of wind turbine blades.Research was limited to the geometry of the rectangular vanes, so it was not possible to explore other geometric profiles that could improve performance or efficiency of flow control for these vanes besides the parametric variations of height and angle that were investigatedThere is no analysis of drag coefficients or momentum loss, ignoring the significance of drag coefficients in relation to the aerodynamic losses caused by vane installation despite benefits related to separation control.
Research Question/Problem/ Need	How do CFD methods change the results of vortex generator CFD simulations?

Important Figures	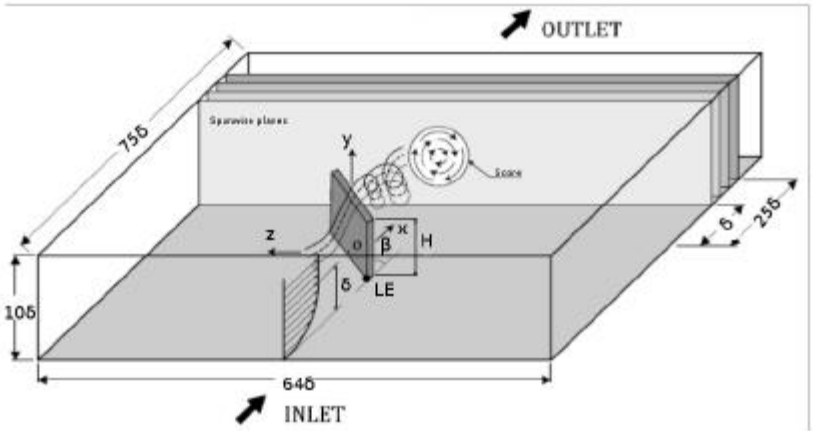 **Figure 1.** Computational domain. 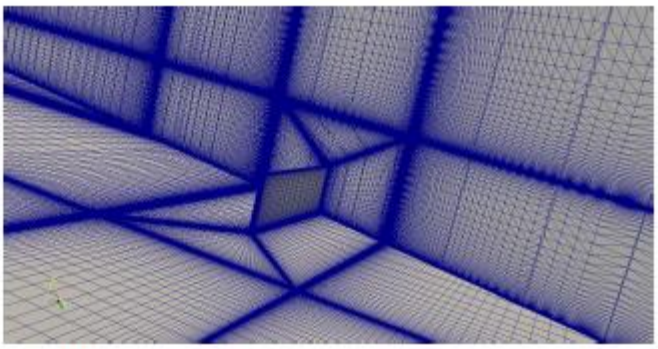 **Figure 2.** Refined mesh sections near the vortex generator (VG).

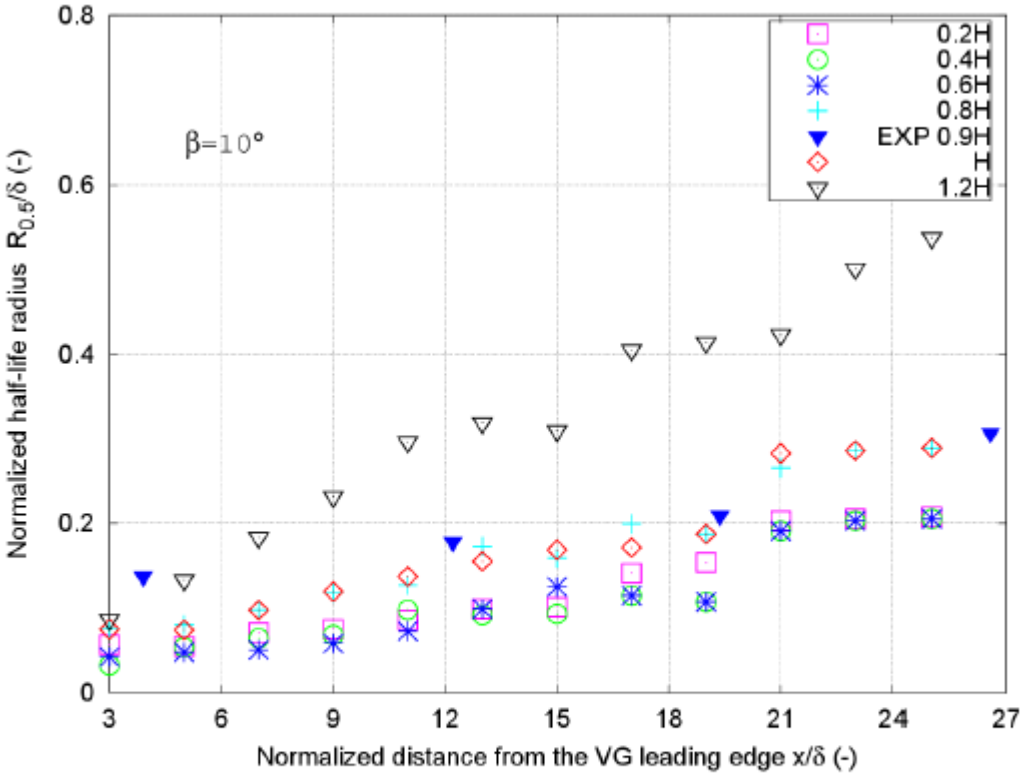

(a)

Figure 7. *Cont.*

VOCAB: (w/definition)

- Half-life radius (R0.5): The distance from the center of a vortex to the point where the rotating motion is half as strong as its peak strength.
- Streamwise vorticity: The spinning motion of fluid that occurs along the direction of the main flow, perpendicular to the vortex axis.
- Non-orthogonality: A measure of how much the angles between mesh cell faces deviate from perfect 90-degree angles, affecting computational accuracy.
- Skewness: A measure of how distorted or stretched mesh cells are, where perfectly square cells have low skewness and heavily stretched cells have high skewness.
- Circulation: The total amount of spinning motion in a vortex, calculated by integrating the vorticity over an area surrounding the vortex core.
- Wall shear stress: The friction force per unit area that the flowing fluid exerts on a solid surface, which increases when the boundary layer is reattached and flowing smoothly.

Cited references to follow up on	None in this one
Follow-up Questions	How would the article's methodology change if the domain was changed from a plate to an airfoil? Why do vortex generators behave differently under different turbulence models?

Article #17 Notes: An overview of flow control in aerodynamic surfaces using vortex generators

Source Title	An overview of flow control in aerodynamic surfaces using vortex generators
Source citation (APA Format)	Jayanarasimhan, K., & Balasubramanian, N. K. (2025). An overview of flow control in aerodynamic surfaces using vortex generators. *Physics of Fluids*, *37*(3). https://doi.org/10.1063/5.0260937
Original URL	https://pubs-aip-org.ezpv7-web-p u01.wpi.edu/aip/pof/article/37/3/031307/3341063/An-overview-of-flow-control-in-aerodynamic
Source type	Journal article
Keywords	Flow control, vortex generators, literature review, fluid dynamics, computational fluid dynamics
#Tags	
Summary of key points + notes (include methodology)	• This literature review summarizes around 2000 research works over a period of five decades, from 1969 till 2024, related to passive flow control using vortex generators on aerodynamic surfaces such as Aircraft Wings & Horizontal Axis Wind Turbines. • It discusses information on computational analysis through RANS, LES, and hybrid techniques, prototype testing using a wind tunnel, as well as field testing of aerodynamic surfaces. • Coverage involves the development of six individual profiles of vortex generators, such as triangles, rectangles, wishbone, trapezoid, delta, as well as gothic shapes that possess distinct vortex creation properties for certain air flows • Many parameters were varied in optimization such as position on the chord, angle of attack, ratio of height to boundary layer thickness, spacing between device pairs, approaches for arranging devices • Performance is measured using lift coefficient, drag coefficient, power coefficient, pressure coefficient, or annual energy production methodologies, with data extracted into detailed design tables • Triangular shapes show great efficiency in various parameters, with 48.7% lift coefficient ratio improvement with 18 degrees of angle of attack, with least drag ratio difference among rectangular, trapezoidal, and other profiles

	• The point of convergence for the optimum chordwise position is at 20 to 30 percent of the chord length, represented by the area of maximum momentum transfer upstream of the naturally occurring separation points for adverse pressure gradients. • Optimum tilt for maximizing the angle of inclination is found at 15° to 18°, after which the adverse pressure gradient leads to a drag crisis verified through at least 15 independent experiments • Height to boundary layer thickness ratio is most effective between 0.8 to 1.5, with heights below 0.8 ineffective for momentum transport, while larger heights impede paths of the flow • Counter-rotating vortex configurations are always preferable to co-rotating vortex configurations in terms of stall delay and boundary layer energy excitation, as downwash is created between the pairs that fixes the flow to the surface. • In adverse pressure gradients for external flows, k-omega SST RANS for turbulence is selected as the preferred form of turbulence closure, coupling k-omega models for the near-wall region with k-epsilon models in the freestream region for better performance. • Code implementations such as DLR TAU models, jBAY source term models, Free Wake Lifting Line models, or Q3UIC codes for viscous-inviscid interactions are used for overcoming shortcomings of production codes, especially for rotational three-dimensional terms or dynamic stalls. • Mod-2 tests by Sullivan et al. showed improvement of 11 percent AEP with devices installed from 20 to 70 percent of the blade span, but no full-scale verification studies were found except for 8 of 206 documented tests that involved experimental verification • Dynamic stall control is not given much attention despite its relevance, with dynamic vortex phenomena mentioned in relation to concepts of deployable devices, but there was no discussion of phase-locked actuation or models of vortex dynamic behavior. • There is no Reynolds number scaling law despite the Re number ranging from 0.03 to 6.1 million, with no dimensionless correlations or scaling laws for extrapolation from laboratory to real-world applications. • The article mainly covers subsonic flows with only a small reference to the transonic or supersonic regimes. • It reveals that there are many key research gaps that remain unsettled until now, including the physics of double-array vortex interactions, unconventional profile performance, non-dimensional optimization techniques, transition of flows at low Reynolds numbers, high-speed vortex interactions for air, effects of air geometry, and others. • Unconventional airfoils including rod vortex generator airfoils, gothic, wishbone, and ogival airfoils look promising for limited operational ranges but are inadequately

	• Some of the key areas that need to be explored include high-fidelity experimental databases for Re over 10 million for large-scale verification, framework development for multi-fidelity optimization that couples low-order models with DNS, aeroelastic properties of Modified Pressure Distributions, and machine learning models for real-time optimization for the Site-Specific Case, as this would greatly improve the fidelity of vortex generator simulations • Findings of systematic RANS simulation errors for vortex persistence prediction imply the potential for physics-informed machine learning to improve computational shortcomings without the computational cost of LES simulations
Research Question/Problem/ Need	How do different computational methods, vortex generator geometries and configurations, applications, and experimental protocols influence their outcomes?
Important Figures	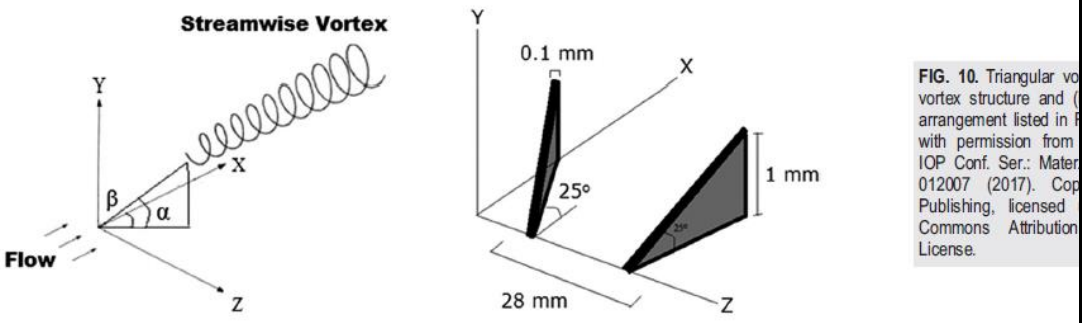 FIG. 10. Triangular vo vortex structure and (arrangement listed in F with permission from IOP Conf. Ser.: Mater 012007 (2017). Cop Publishing, licensed Commons Attribution License.
VOCAB: (w/definition)	• Adverse Pressure Gradient: A region in a flow where pressure increases in the direction of flow, which causes the flow to decelerate and leads to separation from a surface. • Taylor-Gortler Mechanism: The physical principle where a concave surface experiences an incoming flow that naturally creates a vortex stream, and this was used in early vortex generator design. • Horseshoe Vortex: Vortex structure with three components consisting of a bound vortex around the device surface and trailing vortices extending downstream, creating complex momentum redistribution. • Counter-Rotating Arrangement: A vortex generator configuration where paired devices are positioned opposite to each other, creating downwash between them that pins the boundary layer to the surface. • Streamwise Vorticity: The rotational component of flow aligned with the primary flow direction, which is responsible for transferring momentum across the chord and delaying separation.

	• Submerged Vortex Generators (SVGs): Vortex generators embedded within or below the boundary layer that use microjets or specialized geometry to generate vortices without protruding significantly from the surface. • Circulation Strength: A quantitative measure of the total rotational flow magnitude around a vortex • Viscous-Inviscid Interaction Code: A computational method that couples viscous boundary layer calculations with inviscid outer flow solutions, which is useful for vortex generator simulations • Three-Dimensional Rotation Effect (TDRE): The physics phenomenon where rotating blades experience additional forces and altered vortex dynamics compared to static surfaces (applicable for wind turbines)
Cited references to follow up on	W. L. Siauw and J. P. Bonnet, "Transient phenomena in separation control over a NACA 0015 airfoil," Int. J. Heat Fluid Flow 67, 23–29 (2017). O. M. Fouatih, M. Medale, O. Imine, and B. Imine, "Design optimization of the aerodynamic passive flow control on NACA 4415 airfoil using vortex generators," Eur. J. Mech.-B/Fluids 56, 82–96 (2016).
Follow-up Questions	How could vortex generators be improved upon to better serve modern aircraft? What are the deep, underlying issues with vortex generators?

Article #18 Notes: Multi-fidelity machine learning applied to steady fluid flows

Source Title	Multi-fidelity machine learning applied to steady fluid flows
Source citation (APA Format)	Fuchi, K. W., Wolf, E. M., Makhija, D. S., Schrock, C. R., & Beran, P. S. (2022). Multi-fidelity machine learning applied to steady fluid flows. *International Journal of Computational Fluid Dynamics*, *36*(7), 618–640. https://doi.org/10.1080/10618562.2022.2154758
Original URL	https://www.tandfonline.com/doi/full/10.1080/10618562.2022.2154758?scroll=top&needAccess=true
Source type	Journal article
Keywords	Multi-fidelity, fluid flow, Machine learning; small data;multi-fidelity; CFDinitialisation; elliptic inputfeatures
#Tags	
Summary of key points + notes (include methodology)	• This article explores building generalized ML models with minimal training data from very few CFD simulations of varying fidelities • The project aims to run a few expensive CFD simulations early as reference cases, training the ML model on that small dataset and then using the ML model to quickly generate good initial conditions and subsequent design evaluations in hopes of 20-60% less time for the simulations to converge • The authors made a data driven neural network that predicts steady fluid flow fields to speed up CFD simulations • They use a multi-fidelity approach where the model learns the difference between low fidelity and high fidelity simulations to make better predictions • A novel aspect of this research is using elliptic input features instead of Cartesian coordinates to achieve geometry generalization with minimal data. • Elliptic input features are inputs of a potential function, a streamline function and the velocity magnitude rather than x,y,z • The elliptic input features change automatically as geometry changes, making the model automatically aware of the geometry rather than explicitly including design variables in the network • For simple chapes such as cylinders or airfoils, these features can be calculated with conformal mapping

	• Most machine learning based approaches that use cartesian coordinates require embedding the design parameters such as Reynolds number, angle of attack, different geometries as explicit inputs which means that the training data needs to be scattered across an entire design space • EIFs enable different geometries to be predicted for without needing those parameters • The model predicts the discrepancy between low and high fidelity flow field simulations • The neural network has a fully connected network with ten hidden layers, 100 neurons per layer, and sine activation functions to help with smoothness • TensorFlow version 2 was used • Uses as few as 1-2 high fidelity CFD simulations as reference cases • Data points were samples only in a training window, not near the entire body, and the training window size was 30a x 20a where a = radius of a cylinder • The best spot for data size was around 1000 points, based on their tests showing a rapid error drop near m = 1000. • Many training points can be derived from just one high fidelity solution through pointwise evaluation • Results showed that the quadtree sampling consistently gave the best results, especially near the body, uniform and random sampling were seen to have missed some important boundary layer features • Errors increased when the predictions moved away from training conditions such as geometry changes and angles of attack changes • At a 2 degree angle of attack, the speedup was 22% • At a 5 degree angle of attack, the speed up 58% • ML initialization was far less robust on coarse meshed, but it works best on fine meshes • Some other methods that were not used are physics informed neural networks, which incorporate physics equations directly into the training and use PDE residuals as part of the loss function instead of needing lost of simulation data, and they have an unsupervised or semi-supervised approach • Other modes that were not used were CNNs, GNNs, DeepONets, Fourier neural operations, and PointNets because they all require hundreds to thousands of training simulations. As of right now, this method has not demonstrated time dependent flows, unsteady flows, 3D geometries. • This method also does not predict lift and drag coefficients, but only flow fields • ML initialization can sometimes slow down convergence if predictions have errors in critical regions

	• There were no direct comparisons to other ML approaches, other CFD methods, other mesh strategies, but only free stream initialization
Research Question/Problem/ Need	How can multi-fidelity machine learning methods be used to generalize and predict computational fluid dynamics problems? Problem: Running high fidelity CFD simulations is extremely slow and resource intensive.

Important Figures

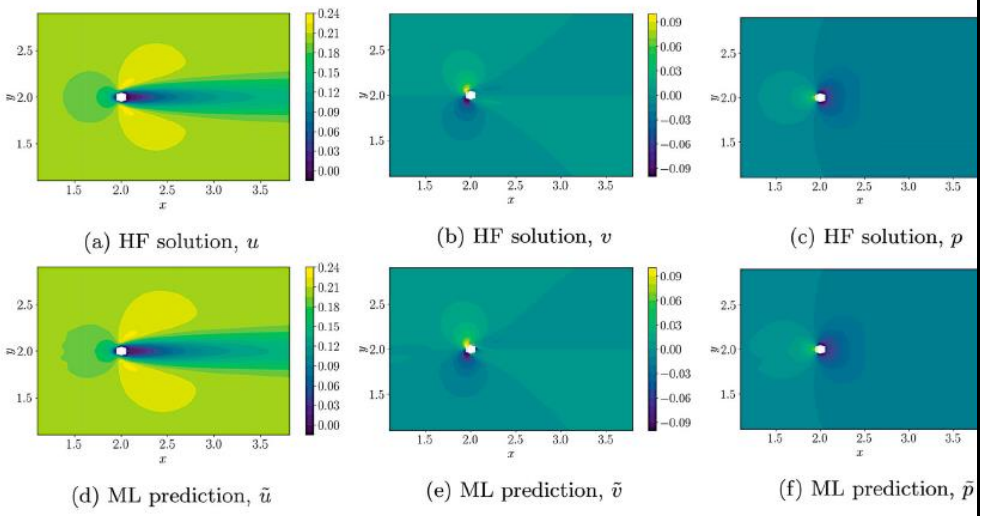

(a) HF solution, u (b) HF solution, v (c) HF solution, p

(d) ML prediction, $\tilde{u}$ (e) ML prediction, $\tilde{v}$ (f) ML prediction, $\tilde{p}$

Figure 10. The trained ML model was used to predict the flow fields at a smaller circular cylinder at R =90% reference rad compared to the HF solution (a–c). (a) HF solution, u. (b) HF solution, v. (c) HF solution, p. (d) ML prediction, $\tilde{u}$. (e) ML predict prediction, $\tilde{p}$.

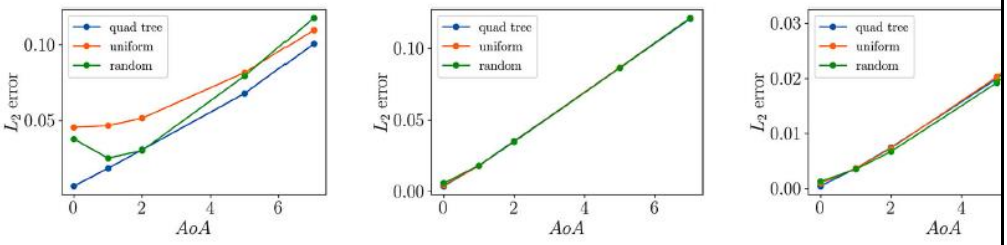

(a) Velocity, x-component (b) Velocity, y-component (c) Pressure

Figure 14. Prediction errors for flow around a Joukowski airfoil using ML models trained at AoA = 0°. Data points were dis (a) uniform, (b) random, and (c) quadtree sampling methods. (a) Velocity, x-component. (b) Velocity, y-component. (c) Pre

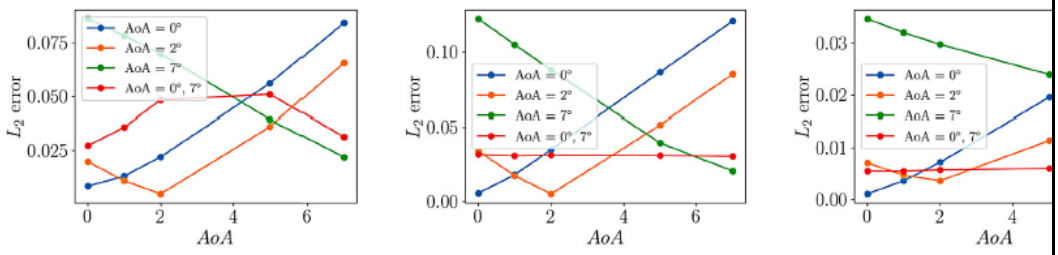

(a) Velocity, x-component (b) Velocity, y-component (c) Pressure

Figure 16. Prediction errors for flow around a Joukowski airfoil based on ML models trained using various reference proble problems with AoA = 0°, AoA = 2°, AoA = 7°, and AoA = 0° and 7°, were included in the ML model training. Data points dis quadtree sampling were used. (a) Velocity, x-component. (b) Velocity, y-component. (c) Pressure.

VOCAB: (w/definition)

- Elliptic Input Features (EIFs): Input features for machine learning models derived from solutions to elliptic boundary value problems (like Laplace's equation) rather than using Cartesian coordinates. These features naturally

	transform with geometry changes, enabling model generalization across different shapes. • Pointwise Evaluation: The process of extracting data values at individual coordinate locations rather than working with entire fields or grids. Used to generate training data by sampling flow quantities at specific points within a domain. • Sobolev Training: A neural network training method that includes derivative information in the loss function, not just function values. Named after Sobolev spaces in mathematics, which measure both functions and their derivatives. • Quadtree Adaptive Sampling: A recursive domain subdivision method that uses a tree structure with four children per node to distribute data points. This method concentrates points in high-gradient regions t • Solver Convergence (Warm-Starting): The process of a numerical solver iteratively approaching the correct solution. Warm-starting means providing a good initial guess to reduce the number of iterations needed, as opposed to cold-starting from uniform or zero conditions. • Conformal Mapping: A mathematical transformation technique that preserves angles between curves. In fluid dynamics, it is used to map complex geometries to simpler ones where analytical solutions already exist, which is possible on airfoils • Function-Type Models: Machine learning models that map individual point inputs to individual point outputs. Contrasts with operator-type models that map entire function spaces to function spaces. • Operator-Type Models: Machine learning models that map entire input fields or functions to entire output fields, rather than individual points. Examples of these include CNNs, graph neural networks, and Fourier neural operators, typically requiring more training data than function-type models.
Cited references to follow up on	Eivazi, Hamidreza, Mojtaba Tahani, Philipp Schlatter, and Ricardo Vinuesa. 2022. "Physics-Informed Neural Networks for Solving Reynolds-Averaged Navier–Stokes Equations." *Physics of Fluids* 34 (7): 075117. doi:10.1063/5.0095270.
Follow-up Questions	Would a model trained at one Reynolds number work at a different Reynolds number? How would the training process and results possibly change when introducing 3D simulations or turbulent flows?

Article #19 Notes: A Machine Learning-Based Approach for Predicting Aerodynamic Coefficients Using Deep Neural Networks and CFD Data

Source Title	A Machine Learning-Based Approach for Predicting Aerodynamic Coefficients Using Deep Neural Networks and CFD Data
Source citation (APA Format)	NEGOITA, M.-F., & HOTHAZIE, M.-V. (2024). A machine learning-based approach for predicting aerodynamic coefficients using deep neural networks and CFD Data. *INCAS BULLETIN*, *16*(4), 91–104. https://doi.org/10.13111/2066-8201.2024.16.4.9
Original URL	efaidnbmnnnibpcajpcglclefindmkaj/https://bulletin.incas.ro/files/negoita_hothazie__vol_16_iss_4.pdf
Source type	Journal article
Keywords	artificial neural network, machine learning, computational fluid dynamics, automation, aerodynamic coefficients
#Tags	
Summary of key points + notes (include methodology)	• This article explores using automated CFD to generate training data then deep neural networks to predict aerodynamic properties as a way to reduce computational costs without sacrificing accuracy • The project aims to eliminate expensive wind tunnel testing and time consuming CFD by training ML models on automated simulation datasets that can instantly predict lift, drag, pressure distributions and skin friction distributions for airfoils • The authors made a fully automated pipeline connecting MATLAB geometry generation, Ansys meshing and SU2 flow solving to create consistent datasets, then trained neural networks to replicate CFD results • They use NACA four digit parametrization reducing the problem to three geometric parameters instead of hundreds of coordinate points • A novel aspect of this research is the decomposition strategy where separate models were created for upper and lower surfaces and for each camber value to reduce complexity and improve accuracy • Maximum camber M controls centerline curvature, camber position P determines where maximum curvature occurs, maximum thickness T defines airfoil thickness as fraction of chord

	• The decomposition strategy divides training by surface and by maximum camber creating twelve total models rather than one massive network, making training faster and generalization better • For distribution predictions the network takes four inputs which are camber position P, thickness T, angle of attack and chordwise position x • Most machine learning based approaches struggle with extreme values at stagnation points and with capturing flow separation, but this approach works well in attached flow regimes by limiting angles of attack to negative four through positive seven degrees • Data normalization with z-score transformation ensures all features contribute equally and prevents magnitude differences from biasing the learning • The neural network for lift and drag uses four inputs which are M, P, T and angle of attack, has two hidden layers and outputs lift coefficient and drag coefficient • MATLAB Deep Learning Toolbox was used • Uses three thousand eight hundred eighty eight total simulations combining six camber values, six camber positions, nine thickness values and twelve angles of attack • The computational domain uses a circular far field boundary placed two hundred fifty chord lengths away with unstructured triangular elements and structured quadrilateral boundary layer mesh • The best performance was around sixteen hundred epochs based on validation error reaching minimum before overfitting began • Training data quality was critical since inconsistent data causes alternating gradients and poor fitting • Results showed R squared above zero point nine nine nine eight for validation indicating exceptional accuracy, and all twelve models achieved R squared above zero point nine nine seven • Errors appeared at extreme values particularly stagnation points for thin airfoils and near leading edge on lower surfaces • At NACA two four one two airfoil at four degrees angle of attack the RMSE was only zero point zero zero one eight five for upper surface pressure • Neural network predictions require no mesh generation, no iterative solver convergence and no turbulence model evaluation • ML predictions were not tested against experimental wind tunnel data but only validated against CFL3D solver • Some other methods that were not explored are more sophisticated parametrization like Bezier curves or class shape transformation, convolutional neural networks to predict full contour fields, physics informed neural networks, ensemble methods, and Bayesian approaches for uncertainty quantification

	• Other applications that were not tested were three dimensional wing configurations, compressible transonic and supersonic flows with shock waves, unsteady separated flows, stall and post stall conditions, real time flight control implementation • This method also does not include transfer learning to new airfoil families, interpretability methods to understand which features drive performance, or integration into gradient based optimization • ML predictions can have issues with extrapolation beyond training ranges, struggle with extreme gradients, and depend fundamentally on dataset size • There were no quantitative comparisons of computational time savings, no disclosed neuron counts or hyperparameters like batch size and learning rate, no discussion of memory requirements, but validation showed predictions closely replicate CFD with drastically reduced time
Research Question/Problem/ Need	How can the computational time of the prediction of pressure lift, drag, and other factors relevant to computational fluid dynamics be reduced while still maintaining the accuracy found in traditional CFD simulations?

Important Figures	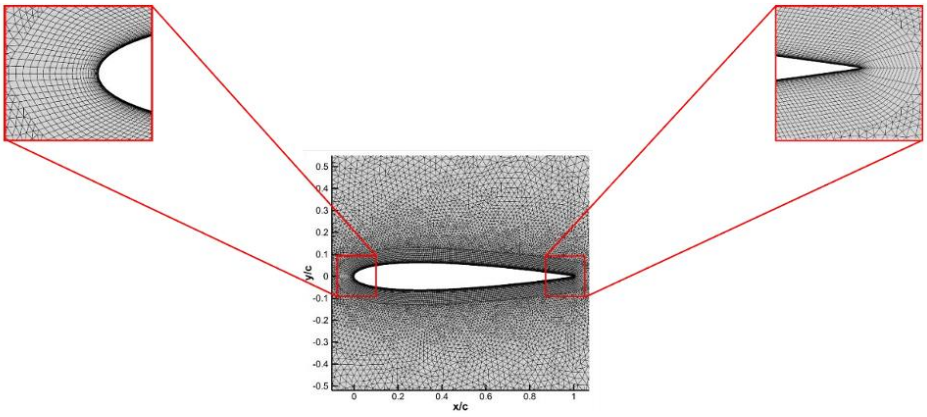 Figure 3. Mesh around the airfoil 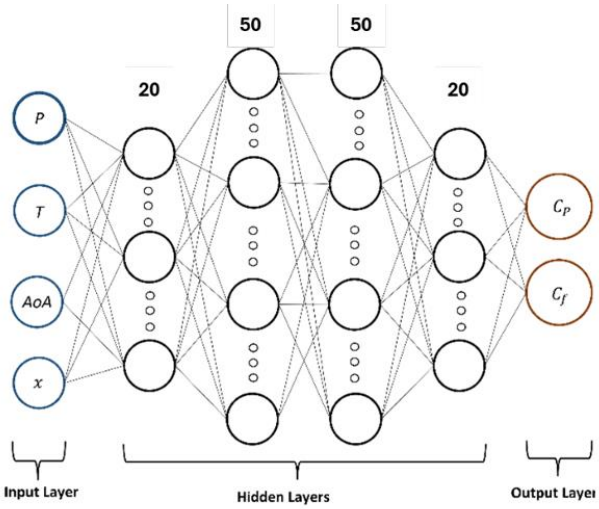 Figure 4. Deep Neural Network architecture for pressure and skin friction coefficients distributions 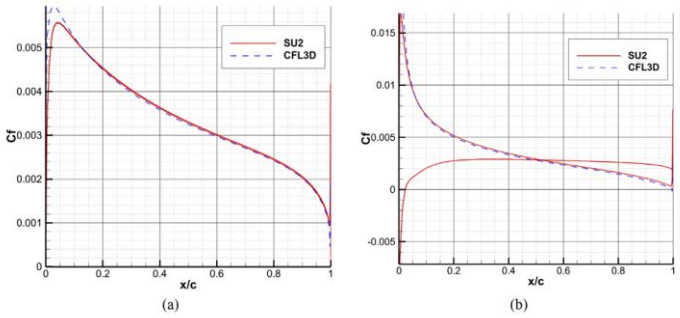 Figure 6. Skin Friction Coefficient Distribution versus Normalized Chord Length at α = 0° (a) and α = 10° (b)
VOCAB: (w/definition)	• Backpropagation: A training technique used with gradient descent where the neural network calculates gradients of the loss function with respect to all weights, then propagates error backward through layers to adjust weights and biases to improve predictions. • Z-Score Normalization: A data preprocessing method that transforms features to have a mean of zero and standard deviation of one

	• Overfitting: A phenomenon where the neural network only replicates previously learned training data without correctly capturing behaviors of unseen data • Spalart-Allmaras Turbulence Model: A one-equation turbulence model used in the CFD simulations for capturing turbulent flows in aerodynamic cases, chosen for balancing computational efficiency with reasonable accuracy. • Y Plus (y+): A dimensionless wall distance parameter critical for boundary layer resolution in CFD simulations, maintained below one across the entire airfoil surface in this study to meet requirements for wall-resolved turbulence modeling. • Hyperparameters: Configuration settings external to the model that control the learning process such as layer counts, neuron numbers, learning rates, and training duration
Cited references to follow up on	None
Follow-up Questions	Would the deep neural network still work for 3D simulations if the approach is fully data driven?

Article #20 Notes: Predicting surface pressure fields and lift coefficients of subsonic airfoils by machine-learning-enhanced compressive sensing framework

Source Title	Predicting surface pressure fields and lift coefficients of subsonic airfoils by machine-learning-enhanced compressive sensing framework
Source citation (APA Format)	Zhang, Y., Zhang, S., Jiang, F., Wu, Z., & Li, W. (2025). Predicting surface pressure fields and lift coefficients of subsonic airfoils by machine-learning-enhanced compressive sensing framework. *Physics of Fluids (1994)*, *37*(9). https://doi.org/10.1063/5.0282416
Original URL	https://pubs-aip-org.ezpv7-web-p-u01.wpi.edu/aip/pof/article/37/9/095103/3361200/Predicting-surface-pressure-fields-and-lift
Source type	Journal article
Keywords	Compressive sensing, subsonic, airfoil, machine learning, CFD, compute time, pressure field, neural network, deep neural network
#Tags	
Summary of key points + notes (include methodology)	• This article introduces a machine-learning-enhanced compressive sensing (ML-CS) framework that synergizes data-driven learning with sparse sensing to predict aerodynamic flow fields and lift coefficients without full CFD simulation • The project aims to overcome the "black-box" nature of traditional surrogate models by integrating physical flow field information into the prediction process, creating a "gray-box" approach that improves accuracy and interpretability • The authors developed a sensor-free prediction pipeline where a Kriging surrogate model first predicts pressure values at specific sparse sensor locations, and then a compressive sensing algorithm reconstructs the entire pressure field from these few points • They use a Singular Value Decomposition (SVD) parametrization method on the UIUC airfoil database, representing geometry through camber and thickness modes rather than direct coordinates or NACA parameters

	• A novel aspect of this research is the "implicit surrogate" strategy for lift prediction, where the lift coefficient is calculated by integrating the reconstructed pressure field rather than mapping geometry directly to lift, reducing errors by thirty-five point five percent • Camber-thickness modes split the geometry into physical attributes, where the first seven modes capture over ninety-seven percent of the geometric energy • The decomposition strategy involves training the sparse basis using Proper Orthogonal Decomposition (POD) on a small dataset of one hundred airfoils, which was found to be more efficient than using a larger dataset due to energy leakage issues • For field reconstruction, the framework utilizes only ten optimal sensor locations determined by Particle Swarm Optimization (PSO), significantly below the Nyquist-Shannon sampling limit • Most compressive sensing approaches require physical sensors, but this method innovates by replacing physical measurements with Kriging-predicted values, making it capable of "sensor-free" prediction for new geometries • Data sampling for geometry uses Latin Hypercube Sampling with a constraint strategy where high-order mode coefficients are bounded by response surfaces of the primary mode to prevent unphysical, wavy airfoil shapes • The neural network and reconstruction algorithms were validated against OpenFOAM RANS simulations using the Spalart-Allmaras turbulence model • Uses a dataset of one hundred subsonic airfoils at a Reynolds number of six million and zero degrees angle of attack • The computational domain employs a structured mesh generated automatically by pyHyp, ensuring consistent node distribution for the POD basis extraction • The best performance was achieved with ten POD modes, as adding higher-order modes introduced small-scale fluctuations that degraded reconstruction accuracy for the testing set • Training data quality was balanced against computational cost, showing that a small high-fidelity dataset of one hundred samples outperformed a lower-fidelity large dataset of one thousand samples for this specific sparse reconstruction task • Results showed a mean relative error of two point four three percent for lift coefficient prediction on the testing set, compared to four point nine two percent for the traditional explicit Kriging model • Errors in pressure reconstruction were most pronounced at the leading edge where pressure gradients are steepest and difficult for sparse sensors to capture

	• At zero degrees angle of attack, the framework achieved greater than ninety-two percent accuracy in pressure coefficient prediction using the virtual sensor scheme • The method allows for detailed flow field visualization and inverse design capabilities that standard scalar-output surrogate models cannot provide • ML-CS predictions were validated only against numerical RANS data and not experimental wind tunnel testing • Some other methods that were not explored include time-resolved sensing for unsteady flows, deep reinforcement learning for sensor placement, or Convolutional Neural Networks for direct field mapping • Other applications relevant to the deployable VG project but not tested include using the reconstructed pressure field to detect flow separation onset in real-time, optimizing VG placement based on the POD mode energy distribution, and using the "sensor failure" resilience for robust active flow control systems • This method does not currently account for varying angles of attack or compressible flow effects where shock waves might alter the sparsity of the pressure field • The sparse reconstruction approach fundamentally relies on the flow field being "compressible" into a few modes, which may be challenged by the complex, chaotic wake structures introduced by deployed vortex generators • There were no quantitative comparisons of memory usage, but the study highlighted that the implicit model required only ten percent of the training data volume of conventional models to achieve superior accuracy
Research Question/Problem/ Need	How can machine learning be used with compressive sensing to create a geometry-informed, sensor-free framework that accurately predicts the surface pressure fields and lift coefficients of subsonic airfoils?

Important Figures	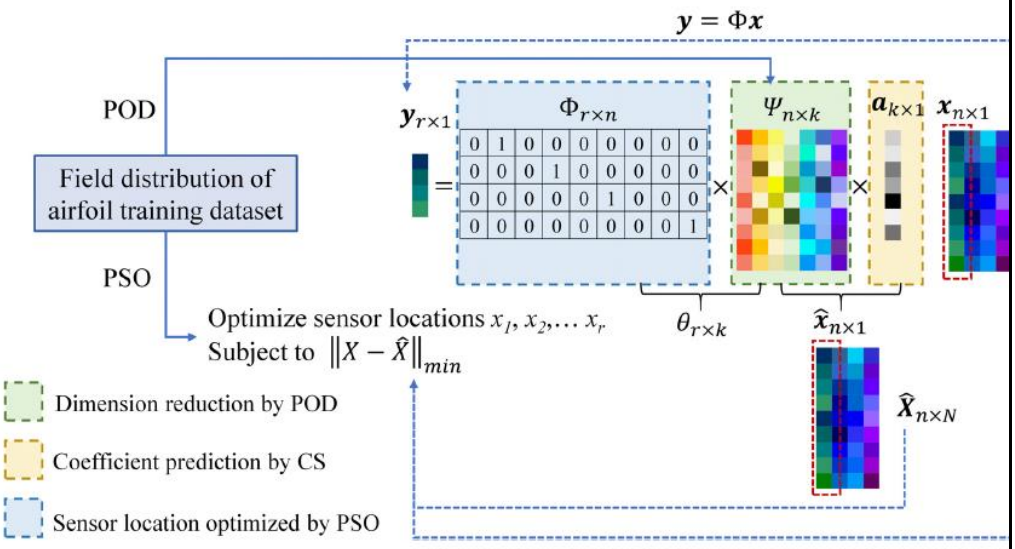 FIG. 7. Schematic of machine-learning enhanced compressive sensing framework applied to the flow field reconstruction of N subsonic airfoils with n g 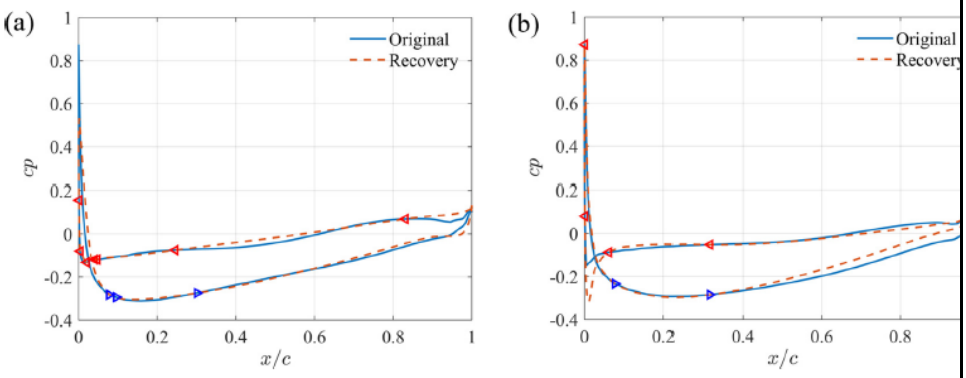 FIG. 16. Comparison of the original and reconstructed cp distribution of airfoil sample with maximum error as (a) $M = 10$, $K = 6$ and (b) $M = 6$,
VOCAB: (w/definition)	• Compressive Sensing: A mathematical technique that reconstructs a complete, detailed dataset (like a full airflow pressure map) using only a very small number of sample measurements, far fewer than traditionally required. • Proper Orthogonal Decomposition (POD): A method used to simplify complex flow data by identifying the most energy-full modes or dominant patterns • Surrogate Model: A fast, approximate model trained to predict the results of a complex, expensive simulation (like CFD) instantly, acting as a "substitute" to save time. • Kriging: A statistical interpolation technique used in this study to accurately predict the "virtual sensor" values on the airfoil surface based

	on known data trends, enabling the system to work without physical sensors. • Sparse Basis: A coordinate system where complex data (like fluid flow) can be represented by only a few non-zero numbers; it acts as the dictionary that Compressive Sensing uses to fill in the blanks.
Cited references to follow up on	Linyang Zhu, Weiwei Zhang, Jiaqing Kou, Yilang Liu; Machine learning methods for turbulence modeling in subsonic flows around airfoils. *Physics of Fluids* 1 January 2019; 31 (1): 015105. https://doi-org.ezpv7-web-p-u01.wpi.edu/10.1063/1.5061693
Follow-up Questions	How would the introduction of complex geometries such as vortex generators impact the performance of POD, which relies on the flow field being representable by only a few variables? Can PSO be used for finding optimal sensor locations on an airfoil?

Article #21 Notes (Patent): Controllable Vortex Generator

Source Title	Controllable Vortex Generator
Source citation (APA Format)	Campbell, D. C. (2002). *Controllable vortex generator* (U.S. Patent No. 6,427,948). U.S. Patent and Trademark Office. https://patents.google.com/patent/US6427948B1
Original URL	https://patents.google.com/patent/US6427948B1/en
Source type	Patent
Keywords	Shape memory alloy, SMA, controlled, closed-loop
#Tags	
Summary of key points + notes (include methodology)	• This patent details a controllable vortex generator (VG) system designed to actively switch between a deployed state for high-lift and a retracted state for low-drag cruise performance. • The primary problem solved is the parasitic drag penalty imposed by conventional, fixed VGs during flight phases where their flow-separation control benefits are not required. • The core methodology relies on a Shape Memory Alloy (SMA), specifically a Nickel-Titanium (Nitinol) alloy, for actuation. • This material exhibits a phase change from a soft, easily deformable martensitic state when cool to a rigid austenitic state when heated, forcefully returning to a pre-defined "memory" shape. • The patent highlights the significant force differential, where the SMA can exert a much stronger recovery force when heated than the spring force used to deform it when cool. • In its main embodiment, the VG fin is mechanically biased into a deflected, vortex-generating position by an external spring steel clip when the system is unpowered. • To retract the device, an integrated electrical resistance heating element heats the SMA fin above its transformation temperature, causing it to stiffen and straighten into a low-drag, undeflected position. • This design incorporates a crucial "fail-safe" feature: in the event of power failure, the SMA cools and the spring automatically returns the VG to its deployed state, ensuring stall protection is always prioritized.

	• The physical construction consists of the SMA fin mounted to a base plate, which is then affixed to the airfoil surface using either adhesives or mechanical fasteners. • The control logic is simple, involving a switch that can be operated manually by the crew or automatically linked to the deployment of other high-lift devices like flaps. • A second embodiment is described that eliminates the spring, instead relying on "free recovery" where the SMA is simply bent into its deployed shape during fabrication and returns to a straight memory shape upon heating. • A third embodiment is also mentioned which uses a different mechanical arrangement to achieve the same effect, illustrating alternative design pathways. • The system's key advantage is its solid-state nature, containing no complex rotating parts, gears, or heavy motors, making it lightweight and reliable for aerospace applications. • Specific quantitative details include the use of a roughly 50% Nickel, 50% Titanium alloy and an annealing temperature range of 400 to 550 degrees Celsius to set the memory shape. • Relevant to the deployable VG project, this patent validates using "smart materials" for actuation and provides a concrete mechanical design for an active system that addresses the cruise drag problem. • The patent does not explore advanced control loops using real-time pressure sensor feedback or AI, presenting a simple binary control scheme. • Potential limitations not fully quantified include the thermal lag (cooling time) required for re-deployment and the continuous power draw needed to keep the VGs retracted during cruise. • Primary applications include installation on aircraft wings just upstream of flaps to manage airflow at high angles of attack while maintaining a clean, efficient aerodynamic surface at high speeds. • This mechanism directly supports the project's goal of an "active" system by providing a concrete, experimentally validated actuation method that fits within thin boundary layer constraints
Research Question/Problem/ Need	Parasitic is caused by static vortex generators at cruise conditons

Important Figures	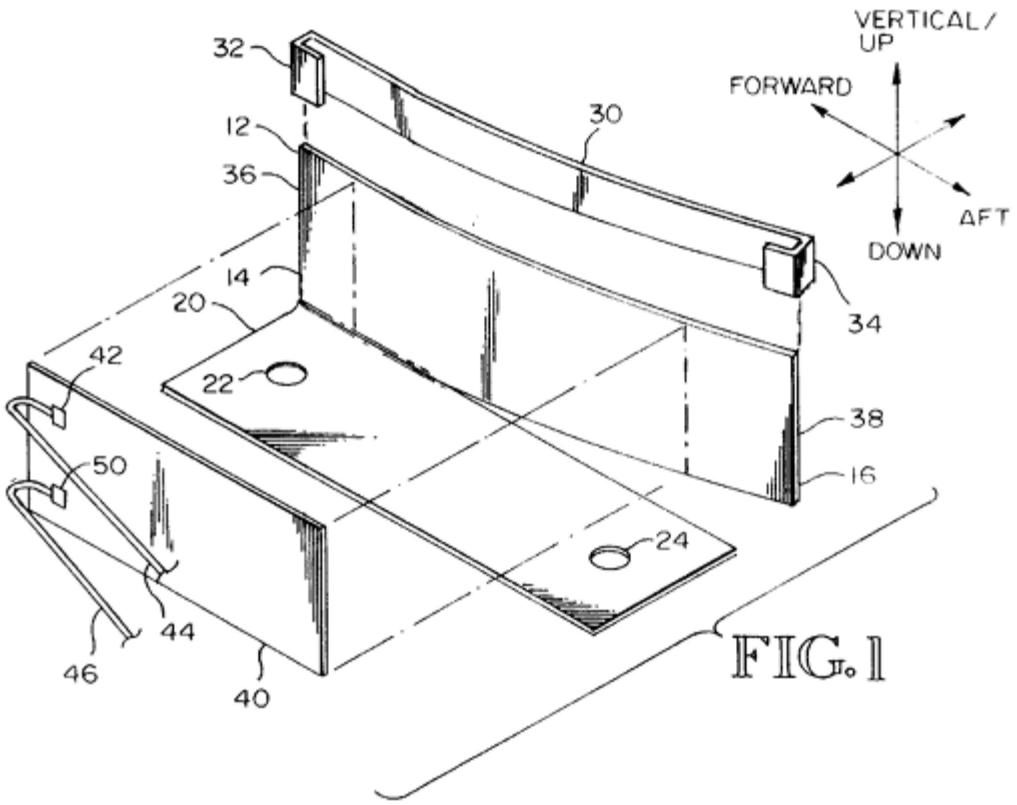 FIG. 1

	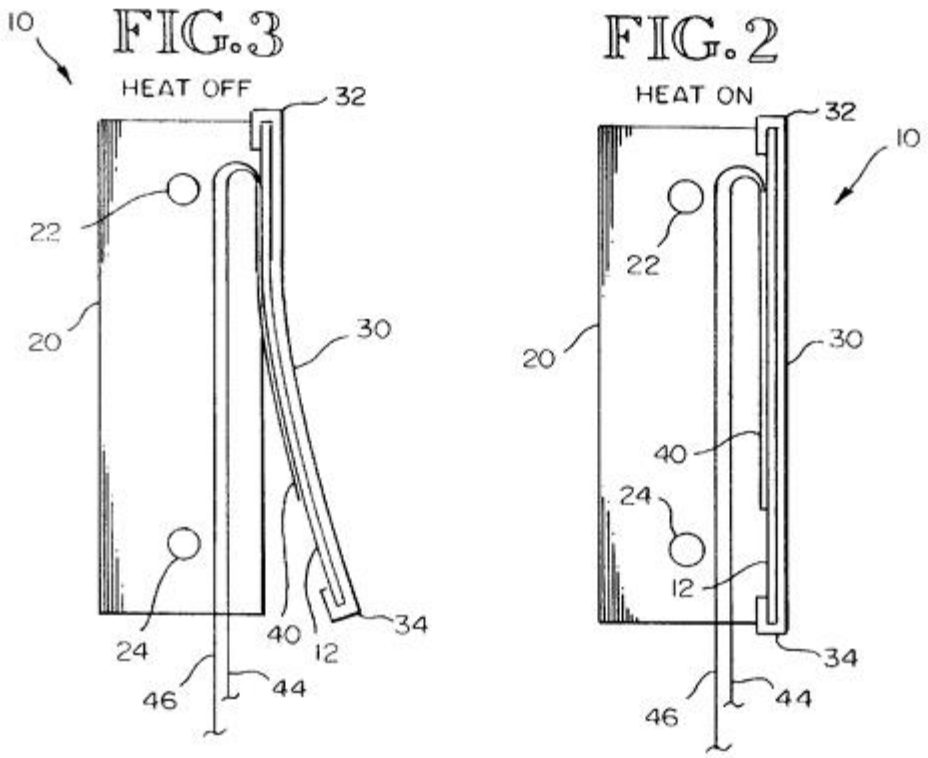
VOCAB: (w/definition)	• Shape Memory Alloy (SMA): A special metal (in this case, Nitinol) that can be bent out of shape when cool and will forcefully return to its original, "remembered" shape when heated. • Transformation Temperature (TTR): The specific temperature at which a Shape Memory Alloy undergoes a phase change, either becoming stiff to recover its shape (when heated) or soft enough to be deformed (when cooled). • Austenite: The crystalline phase of a Shape Memory Alloy at high temperatures; this is the strong, rigid parent phase where the material holds its "memory" shape. • Martensite: The crystalline phase of a Shape Memory Alloy at low temperatures; this is the soft, easily deformable phase that allows the material to be bent into a temporary shape.
Cited references to follow up on	https://patents.google.com/patent/US5662294A/en?peid=64658a69b9380%3A312%3A4763e2d8

	https://patents.google.com/patent/US4039161A/en?peid=64658a7680b40%3A32d%3A5fa0f0c2
Follow-up Questions	What are the key issues that prevented this from being integrated into the world?

Article #22 Notes (Patent): VORTEX GENERATORS RESPONSIVE TO AMBIENT CONDITIONS

Source Title	VORTEX GENERATORS RESPONSIVE TO AMBIENT CONDITIONS
Source citation (APA Format)	Clingman, D. J., Tillotson, B. J., Bordoley, A., & Wang, M. C.-H. (2019). *Vortex generators responsive to ambient conditions*.
Original URL	https://patents.google.com/patent/US9789956
Source type	Patent
Keywords	Passive control, no actuator, adaptive control
#Tags	
Summary of key points + notes (include methodology)	• This patent describes a completely passive, autonomous vortex generator (VG) system that deploys and stows itself based on changes in ambient environmental conditions, specifically temperature and pressure. • The primary problem addressed is the mechanical complexity, weight, and failure risk associated with active actuation systems (motors, solenoids) while still solving the "parasitic drag" issue of fixed VGs. • The core methodology uses a sealed volume of "temperature sensitive material" (like a wax, gas, or phase-change fluid) that expands or contracts with altitude and temperature changes to drive the VG movement. • In one embodiment, a sealed bladder or piston filled with this material expands as the aircraft climbs (due to lower outside pressure) or cools (due to lower outside temperature), driving the VG into a retracted position for cruise. • Conversely, as the aircraft descends to lower altitudes (higher pressure/temperature) for landing, the material volume contracts or is compressed, allowing a bias spring to force the VG into the deployed position. • This design cleverly aligns the "deployed" state with low-altitude, high-lift phases (takeoff/landing) and the "stowed" state with high-altitude, high-speed cruise, perfectly matching the aerodynamic requirements without any computer control.

	• Mechanical linkages translate the linear expansion of the actuator into the rotation or translation of the VG blade, often using simple pivots or cam followers to minimize parts count. • The system includes a manual override or "lock-out" capability in some designs, allowing maintenance crews to force the VGs into a deployed state for inspection on the ground. • Quantitative triggers are discussed, such as designing the system to fully retract above a specific altitude (e.g., 10,000 feet) or below a specific temperature, effectively automating the cycle based on flight profile. • Unlike the previous Shape Memory Alloy patent which used electricity to create heat, this invention harvests the natural cold of high-altitude flight to trigger the shape change, requiring zero electrical power. • A specific embodiment describes a "rotational" deployment where the VG blade pivots out of a recess in the wing skin, which is mechanically simpler to seal against moisture and ice than a sliding piston. • The patent explicitly mentions the use of "bi-metallic strips" (like in old thermostats) as another potential passive motive force, twisting the VG in response to temperature changes. • Relevant to the deployable VG project, this patent challenges the assumption that "active" control requires electricity; it validates that environmental cues (pressure/temp) can be reliable proxies for flight phase (cruise vs. landing). • However, a limitation for "smart" control is that this passive system cannot react to dynamic stall conditions (like a sudden high-G maneuver at altitude) because it is not robust to slow-changing ambient variables.
Research Question/Problem/ Need	Actuation and control methods of active flow control bulky and unwieldy.

Important Figures	

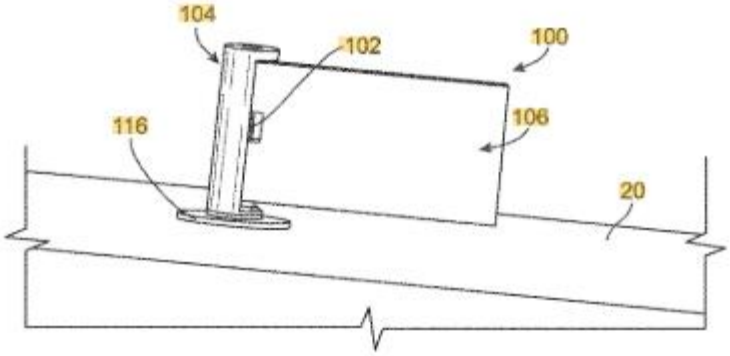

FIG. 1A

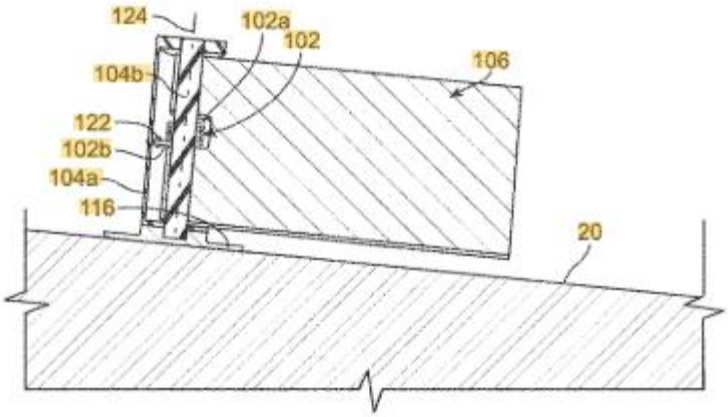

FIG. 1B

	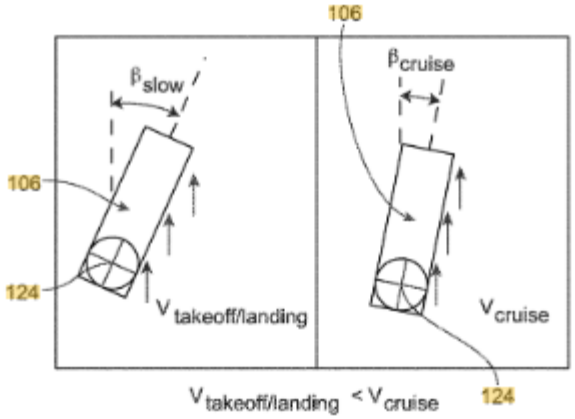 **FIG. 1G** 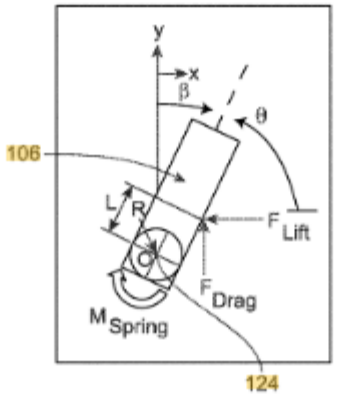 **FIG. 1H**
VOCAB: (w/definition)	• Volume Changing Material: A substance (like paraffin wax or a specific gas) chosen because it significantly expands or contracts when heated or cooled • Aneroid Bellows: A sealed, flexible metal container (often like an accordion) that expands and contracts in response to changes in outside air pressure • Bi-Stable Mechanism: A mechanical design that has two stable resting positions (fully up or fully down) and resists staying in the middle • Bias Member: A simple component, usually a spring, that constantly pushes the device in one specific direction (• Ambient Condition Responsive: Describes a system that reacts automatically to the surrounding environment (like air pressure or temperature) rather than waiting for a command from a computer or pilot.

Cited references to follow up on	None
Follow-up Questions	What are the limitations of a passive system vs. active system when deployed in real life? What would the latency of a passive system be, and why would it matter?